ORIGINAL RESEARCH **Open access**

Performance Assessment of GNSS Error Bounding in Specific Category UAS Operations

Victor Santos[1*], Ana Beatriz[2], Joaquim Dias[1], Ricardo Alves[3]

Abstract

The expanding application of UASs in complex operations, including Beyond Visual Line of Sight (BVLOS) flights and sorties over densely populated areas, has heightened the need for robust navigation integrity. In this setting, GNSS commonly serves as the primary positioning means, though its reliability can be undermined by numerous degrading factors, particularly in cityscapes or confined spaces. This article delves into the consequences of employing GNSSs as an outsourced capability in SAIL III activities, centering on Operational Safety Objective (OSO) #13, as specified in the Specific Operations Risk Assessment (SORA) 2.5. An examination of the stipulations of SORA 2.5 is presented, followed by trials of GNSS data collection across varied settings using receivers from both premium and mid-tier categories. A range of performance metrics furnished by the receivers, such as Dilution of Precision (DOP), Carrier-to-Noise Density Ratio (C/N0), estimated accuracy, and PLs, are scrutinized to gauge their ability to detect navigation deterioration in real time. The outcomes reveal that Protection Levels outperform alternative indicators in pinpointing degradation under demanding circumstances, highlighting the existing shortcomings of GNSS-reliant navigation oversight for specific category UAS undertakings.

Keywords UAS, GNSS, SORA 2.5, SAIL III, OSO#13, Navigation integrity

*Correspondence:
Victor Santos
victor.santos@fc.up.pt
[1] Department of AI for Cork Oak and Chestnut Tree Health Monitoring, Faculty of Agriculture, University of Porto, Porto, Portugal
[2] Department of Machine Learning for Pesticide Reduction and Biological Control, Faculty of Agriculture, University of Campinas, Campinas, Brazil
[3] Department of Smart Forest Fire Risk Prediction, Faculty of Agriculture, University of Coimbra, Coimbra, Portugal

Introduction

The proliferation of UASs is accelerating across a range of fields, including logistics, precision agriculture, infrastructure inspection, and crisis response, driven by rapid technological advances and the need for effective aerial operations. Industry predictions estimate that the UAS market will reach USD 69.9 billion by 2030 [1], while the commercial UAS niche alone is forecast to grow from USD 9.39 billion in 2022 to close to USD 41.78 billion by 2030 [2].

Such market trends indicate both growing capital investment in UAS technologies and the embedding of autonomy-supporting functionalities such as Artificial Intelligence (AI) [3, 4], sensor fusion [5], and 5G communications [6], clearing the path for upcoming operational paradigms, including BVLOS and fully self-governing missions.

In this arena, the positioning apparatus is one of the most vital elements for allowing a broader array of autonomous undertakings. GNSS-grounded navigation remains the primary positioning strategy for UAS operations, appreciated for its cost-effectiveness and worldwide accessibility. Even so, GNSSs remain vulnerable to spoofing, multipath interference,

This is an open access article distributed under the terms of the Creative Commons Attribution-NonCommercial-ShareAlike 4.0 International License (CC BY-NC-SA 4.0), which permits non-commercial use, distribution, reproduction, and adaptation in any medium or format, provided that appropriate credit is given to the original author(s) and source, a link to the license is provided, and any changes made are indicated. Adapted material must be distributed under the same license.

© 2023 The Author(s). | Published by Agro Intelligence Research Press

and signal blockage, especially in urban or low-elevation environments [7]. Each of these impairments gravely weakens navigation integrity, as will be illustrated throughout this work.

Given the pivotal role of GNSSs as the core source for UAS positioning, it becomes imperative, contingent on the hazard level associated with the planned undertaking, to monitor the Position, Velocity, and Time (PVT) solution's efficacy in real time and issue an alert if it proves unfit for use. To address this, the notion of navigation integrity is proposed, defined as the degree of confidence in the soundness of the PVT solution [8]. This idea has previously been matured in airborne navigation apparatus, where a benchmark has long been codified (DO-229) [9] using GPS supplemented by Satellite-Based Augmentation Systems (SBASs).

Over the past few years, several scholarly inquiries have addressed this subject, developing algorithms to enhance both the capabilities and the integrity of GNSSs. Within this framework, multiple RAIM (Receiver Autonomous Integrity Monitoring) algorithms have been put forward, classifiable into three groupings: error probability distribution modeling, set representation techniques, and strategies rooted in machine learning [10]. Time-honored RAIM approaches, including residual-based and solution-separation RAIM, have historically provided the foundation for PL calculations in GNSS integrity surveillance [11]. In cityscapes or hindered settings, the efficacy of RAIM and ARAIM (Advanced RAIM) falls off markedly due to limited satellite line-of-sight [12]. To mitigate these drawbacks, Vision-Aided RAIM (VA-RAIM) has been advanced to bolster integrity monitoring output during phases of diminished visibility, such as approach and touchdown [13]. A further propitious progression is Kalman Filter RAIM tailored for the GNSS/Inertial Navigation System (INS) employing range-domain articulation, which achieves PLs within 10 m of solution-separation RAIM at least 95% of the time [14].

Within Europe, the SORA schema, endorsed by the European Union Aviation Safety Agency (EASA) as an Acceptable Means of Compliance (AMC) [15], serves as the bedrock risk appraisal methodology for UAS operations in specific categories, such as BVLOS or flights above crowds. EASA has already ratified SORA 2.5 [16], which introduces several modifications relative to the preceding edition. SORA presents various hurdles in the enactment of OSOs, as the role of GNSSs remains incompletely delineated.

The present work pursues a twofold aim: the primary aim is to scrutinize the specifications laid down by the distinct OSOs within SORA 2.5 and their implications for GNSSs across SAIL III activities, whereas the secondary aim is to present real-world GNSS data capture efforts spanning diverse settings and to interpret the findings. The closing remarks draw broad conclusions on how GNSSs might be harnessed to meet the requirements laid down in SORA 2.5 and, with greater specificity, on how GNSS sensors can be supervised during operations. This effort was executed by affiliates of the European Organisation for Civil Aviation Equipment (EUROCAE) WG-105 SG-6 [17], whose purpose is to develop benchmarks and directives for the use of GNSSs in UASs and related systems as they evolve to conform to the regulatory landscape. This undertaking serves as a counterpart to a guidance document currently being prepared, with a projected release at the beginning of 2026, meant to establish a methodological approach for deploying GNSSs in SAIL III undertakings.

This study is divided into four sections. Segment 1 furnishes a wide-ranging preamble to the matter under discussion. Segment 2 provides an overview of SORA 2.5, focusing on the OSOs that carry particular weight for GNSSs. Segment 3 lays out the acquired outcomes from GNSS data gathering in contrasting environments, both stationary and in motion, and unpacks the findings. Segment 4 encapsulates the deductions and proposals for tracking GNSSs while airborne within the specific SAIL III operations category.

SORA 2.5

Within the present European regulatory landscape, civil UAS activities are sorted into three distinct classifications [18], dictated by their associated hazard thresholds:

© 2023 The Author(s). | Published by Agro Intelligence Research Press

· ‘Open’ classification: Governs civil drone undertakings of reduced hazard, wherein safety is maintained as long as the civil drone pilot satisfies the pertinent stipulations for the planned activity.

· ‘Specific’ classification: Encompasses civil drone undertakings carrying elevated hazard, with safety upheld by the drone pilot procuring an operational clearance from the national oversight body ahead of commencing the activity. Here, performing a hazard appraisal is obligatory.

· ‘Certified’ classification: The safety hazard reaches a notably high magnitude; thus, credentialing of the drone pilots alongside their aircraft, together with remote pilot licensing, remains mandatory at all times to preserve safety.

Zeroing in on the ‘Specific’ classification, four avenues exist for carrying out flights or attaining flight clearance from the oversight authority, typically the National Aviation Authority (NAA) or EASA:

· Present a declaration anchored to a Standard Scenario (STS).

· Procure an operational clearance in line with a Predefined Risk Assessment (PDRA).

· Procure or function beneath a Light UAS operator Certificate (LUC).

· Procure an operational clearance utilising SORA as an Acceptable Means of Compliance.

The opening avenue corresponds to those activities that fall inside the bounds of the currently established Standard Scenarios: STS 01—VLOS over a supervised terrestrial zone within a populated area; and STS 02—BVLOS utilizing Airspace Observers over a supervised zone. Across both scenarios, the restrictions governing these standard undertakings are stipulated.

The subsequent avenue pertains to those activities for which EASA has previously undertaken hazard appraisal and disseminated the AMC. In this instance, EASA has made five PDRAs available, the bulk of which focus on agricultural or aerial surveillance applications.

Turning to the third avenue, procuring an LUC, the operators must show the NAA that they possess the capability to appraise the hazards intrinsic to their activities autonomously. Should it be conferred, it carries specific prerogatives, chief among them the capacity to execute activities within the classification without requiring operational sanction from the NAA, contingent upon the LUC’s scope restrictions. Under the LUC, the UAS operator is permitted to carry out only the activities defined in the LUC’s conditions of approval; accordingly, for novel activities posing a dissimilar hazard or undertaken in new locales not endorsed in the LUC, the UAS operator must petition for flight authorization. Attaining an LUC is especially critical or beneficial for activities intended to be carried out repeatedly over time.

The concluding avenue covers activities within the specific classification that do not align with any of the preceding alternatives. It is the one demanding the greatest quantity of supporting evidence, as the UAS operator must execute a hazard evaluation of the intended activity in accordance with the SORA methodology, put into effect all required mitigations, and produce the entirety of documentation and substantiation needed to petition for flight clearance from the NAA.

Homing in on this concluding alternative, which accounts for the preponderance of activities to be undertaken within the specific classification, a SORA examination becomes necessary to assess the operational hazard and identify the operational demands. SORA represents a methodology crafted to furnish a hazard-commensurate scheme for ascertaining the evidence and assurance essential for a UAS to attain an acceptable degree of safety within the ‘Specific’ classification. It methodically evaluates operational hazards, setting forth both GRC (Ground Risk Class) and ARC (Air Risk Class), and pinpoints operational requirements to meet the Target Level of Safety (TLOS). What emerges from a SORA is the sorting of the operational hazard into one of six hazard gradations designated SAIL (Specific Assurance and

© 2023 The Author(s). | Published by Agro Intelligence Research Press

Integrity Levels). SAIL I signals the least hazard gradation; SAIL VI indicates the utmost hazard gradation within the specific classification. The SAIL directs the operational demands, embodied as OSOs. At the time this work was published, EASA, which is responsible for shaping the regulatory architecture at the pan-European level for UAS activities, had formally embraced SORA 2.5, formulated by the Joint Authorities for Rulemaking on Unmanned Systems (JARUS) and published in May 2024. SORA 2.5 specifies 17 OSOs, setting out a succession of operational stipulations, together with the proof to be provided to secure operational clearance. OSOs traverse varied spheres and actors, including the UAS designer, UAS operator, and other bodies involved in maintenance, training, or ancillary services. Contingent upon the SAIL gradation, every OSO carries a distinct robustness rating, which may be Not Required, Low, Medium, or High, imposing tighter stipulations as the robustness rating climbs.

Set against this milieu, this paper scrutinizes the role of GNSSs in SORA 2.5 and highlights the obstacles that must be addressed for their sound use within this specific classification. GNSS is an integral component of UAS operations, encompassing both the on-board receiver and external sources (i.e., satellite transmissions from various GNSS constellations). Because of this duality, the GNSS must be regarded under both lenses: as a constituent of the UAS and as an exterior provision underpinning the undertaking. These dual dimensions of GNSSs are profoundly intertwined. Indeed, the UAS/GNSS antenna location is not directly handed over from the exterior system; rather, it is computed on board by the UAS using intelligence supplied by the exterior system.

In keeping with the ambit of the paper, the examination shall be directed at SAIL III, the SAIL gradation for which EASA is currently devising an MoC (Means of Compliance), and which commands a noteworthy commercial stake. Additionally, the stipulations and OSOs about GNSSs remain unchanged across higher SAIL gradations. That said, the requisite robustness rating could alter in kind. A good many distinct OSOs relate to the GNSS straightforwardly or circuitously, yet the ones carrying the greatest weight are as follows:

- OSO#5: The UAS is engineered with due regard to system safety and dependability.
- OSO#8: Operational protocols are laid down, corroborated, and stringently observed.
- OSO#13: The exterior provisions buttressing UAS activities prove suitable for the undertaking.
- OSO#23: The ambient parameters for safe activities are laid down, capable of measurement, and stringently observed.
- OSO#24: The UAS is engineered and validated for hostile ambient parameters.

Amid these OSOs, a portion lies wholly under the producer's purview (OSO#5 and OSO#24), others under the UAS operator's purview (OSO#13 and OSO#23), and, in select instances, answerability is split across both actors.

OSO#05 centers upon making certain that the share of the UAS, or any exterior system buttressing the activities, in the forfeiture of command over the operation within the operational volume stays proportionate to the tolerable hazard threshold connected to each SAIL. In December 2024, EASA issued an MoC for this OSO, applicable to SAIL III [19], that outlines how the stipulations associated with OSO#5 may be met. This publication sanctions the utilization of ED-280 [20] as a touchstone for executing the safety evaluation.

OSO#8 focuses on the specification and verification of operational protocols for handling routine, irregular, and urgent situations that may arise from equipment failures or lapses in human performance. In SORA 2.5 Annex E, inside the Level of Integrity tabulation for this OSO, the necessity to single out the exterior systems buttressing the activities and the compulsion to keep a check on these exterior systems to pick up on slippage in their functioning are inscribed.

As for OSO#23 and OSO#24, each emphasizes the ambient parameters for safe undertakings. In this respect, OSO#23 is tasked with defining the limits of ambient parameters (such as gusts or rainfall) that support safe operations. In contrast, OSO #24 is tasked with ensuring that the UAS, along with its subsystems, is validated to operate within those

© 2023 The Author(s). | Published by Agro Intelligence Research Press

limits. In December 2024, EASA issued an MoC for OSO#24 [19] that guides on meeting the requirements for hardware validation.

OSO#13 is tasked with setting out the stipulations bound up with the exterior provisions buttressing the undertaking. Within SORA 2.5 Annex E, a selection of exemplars of exterior provisions, such as communication utilities, Unmanned Aircraft System Traffic Management (UTM) service facilitators, and GNSSs, is provided. The central thrust of this OSO is, at the outset, to articulate the requisite performance benchmark for these exterior provisions and, subsequently, to monitor their performance in real time and to implement appropriate fallback steps should they degrade.

Within this setting, demonstrating conformance with OSO#13 can be a stiff test for UAS operators, given that the GNSS does not exactly align with the stipulations of this OSO as spelled out in SORA 2.5. To come to grips with how to place GNSS provisions within the purview of OSO#13, the subsections that follow address several foundational questions. In Section 3, real-world GNSS sensor data captured in dissimilar environments are showcased and dissected to address these challenging tests.

Does GNSS service fall under the scope of OSO#13?

SORA 2.5 Annex E, within the Level of Assurance matrix for OSO#13, establishes that this particular OSO is only pertinent to those ‘services critical for the safety of the flight’. The text goes on to characterize such critical services as ones whose loss would directly lead to a loss of control of the operation, as identified per OSO#05. A pair of substantial issues surfaces at this stage.

What ought to be counted as a loss of service is the first matter requiring clarification. Within SORA 2.5, no formal account of service loss is supplied. Turning to the concrete case of GNSS provision, its role is to determine the UAS position; consequently, the notion of a lost service ought to stretch beyond the mere vanishing of satellite signals to encompass signal-corrupting effects that drive positioning error past the threshold tolerated by the planned undertaking.

Whether a GNSS service loss, as just described, would inevitably result in a loss of operational control constitutes the second matter requiring attention. SORA 2.5’s Main Body, more specifically Section 2.3.2, spells out the meaning of an operational loss of control. It should likewise be recalled that the SORA framework, in its entirety, relies on knowing the UAS’s position to derive the GRC and the ARC, making the positioning subsystem indispensable for UAS sorties not conducted under the direct manual command of the remote crew. In these sorts of operations, the question becomes what fraction of the overall positioning chain is owed to the GNSS sensor, recognizing that a UAS will typically rely on a fused positioning arrangement that pulls from multiple sensing devices, such as an Inertial Measurement Unit (IMU) alongside the GNSS. Where such fused architectures are employed, just how essential GNSS proves to be would depend on the extent to which GNSS degradation propagates through the entire positioning chain.

Defining the GNSS service performance threshold

A further major obstacle to the application of OSO#13 to GNSS provision is the question of how to quantify the service’s performance. Per the description found in SORA 2.5 Annex E, OSO#13 sets down a trio of principal demands underpinning the level of assurance:

· The petitioner is tasked with guaranteeing that the external provision’s performance meets the demands of the planned undertaking.

· The petitioner possesses the wherewithal to track, while the mission unfolds, how well these external provisions are functioning.

· Should the live performance threaten to precipitate an operational loss of control, the petitioner institutes suitable countermeasures.

© 2023 The Author(s). | Published by Agro Intelligence Research Press

Taken together, these demands require specifying the yardstick by which GNSS provision performance is measured, thereby setting the minimally acceptable performance for the planned undertaking. As has already been pointed out, GNSS provides the UAS's location. The provision itself, notwithstanding, does not directly yield a position fix; rather, it supplies a collection of satellite waveforms that the GNSS sensor leverages to compute its antenna's coordinates, a fact that renders isolating the provision from the sensor inherently problematic. Selecting which indicators to use for performance measurement is the necessary first step toward specifying GNSS provision performance. Two broad pathways present themselves (an explanation of each of these indicators appears in Section 3):

· Signal in space (SiS) indicators: Figures issued by the receiver that speak to the quality of the SiS (e.g., Signal-to-Noise Ratio), along with the tally of visible spacecraft and their spatial distribution (DOP).

· Sensor-derived indicators: Figures generated by the algorithmic core of the positioning sensor, suitable for live oversight of the positional fix to safeguard the sortie. These incorporate the spacecraft geometry and all contributing error sources, generally providing a statistical envelope or benchmark for the positional deviation (e.g., Protection Levels or Position Error estimation).

Given that OSO#13 focuses on external provisions, the underlying premise is to surveil them as independent entities. As of the drafting of this paper, a UAS-specific GNSS provision has yet to materialize, and the currently fielded GNSS offerings (e.g., GPS, Galileo, EGNOS…) do not equip UAS operators with a dedicated capability to meet the OSO#13 demands outlined earlier. The upshot is that, at this juncture, bridging the gap between the previously cited provision-side indicators and the actual positioning error remains beyond reach. The following section presents a series of data captures illustrating the behaviors exhibited by the referenced indicators.

Analysis of GNSS Data Capture Campaigns

The foremost objective of the present study is to draw on genuine GNSS data captures to demonstrate how GNSS may be harnessed to meet the previously enumerated demands, and to pinpoint the principal indicators that warrant continuous in-flight surveillance for performance evaluation.

Working toward this goal, a set of data-capture campaigns was orchestrated across disparate environmental conditions, with the intent of portraying the categories of signal compromise a GNSS may be subjected to and the effects on its operational fitness. To obtain true positioning deviations, a reference truth was constructed using a Post-Processing Kinematic (PPK) procedure, in which the high-grade receiver logs its own location and observations from a surveyed fixed reference station are folded in. This approach to generating the reference truth was uniformly adopted for both stationary and moving trials, as it furnishes a dependable reference trajectory accurate to the centimeter level. The data capture campaigns carried out are comprised of the following:

· Stationary trials: Experiments wherein various sensors were situated at a surveyed, fixed point were performed across differing settings marked by distinct origins of signal compromise. Each trial lasted a full 24 hours.

○ Nominal Scenario: A setting wherein the UAS traverses an unobstructed sky and the Signal in Space remains free of anomalies.

○ Ionospheric disturbance scenario: A setting in which heightened ionospheric activity exerts an influence on GNSS-derived positioning. Scenarios involving tropospheric disturbance were set aside, owing to their relatively modest contribution to GNSS positioning degradation.

○ Multipath scenario: A setting wherein the UAS operates in a metropolitan locale in proximity to tall structures, lacking an unimpeded line of sight to the GNSS spacecraft.

© 2023 The Author(s). | Published by Agro Intelligence Research Press

○ Multipath + Ionospheric disturbance scenario: A setting where the two degraded conditions manifested simultaneously.

○ L1 Interference scenario: A setting in which an unwanted emission within the L1 frequency band couples into the receiver, degrading GNSS positioning capability.

· Trials involving movement: Testing performed with sensors mounted aboard a UAS while traversing different environmental settings, with varying lengths of data collection.

Every experimental run shared an identical configuration baseline: positioning referenced to World Geodetic System 1984 (WGS84), a 5° cutoff angle for satellite visibility, data logged at 1 Hz intervals, dual-frequency tracking employing L1/L2 for GPS (save for instances where EGNOS was active) together with E1/E5 for Galileo, while the Least Squares algorithm handled position computation. The investigation focused on GPS and Galileo—the two constellations recommended in European aviation regulatory and standards documentation. A total of four distinct sensing devices were utilized across the aforementioned trials. Three represent units commonly deployed in UAS applications, their Size, Weight, and Power (SWaP) profiles being compatible with on-board installation constraints. The fourth device, a unit holding aviation certification, served purely as a comparative benchmark:

· Premium-grade unit: This label designates a high-precision GNSS receiver built for scenarios that demand exact positional fidelity and reliability. By exploiting signals broadcast by multiple satellite constellations and sophisticated processing algorithms, these devices maintain precise, trustworthy positioning even under challenging environmental conditions. An on-board integrity monitoring function (compliant with DO-229 when SBAS correction data are present) computes Protection Level bounds for both horizontal and vertical dimensions and can issue a warning whenever a computed Protection Level breaches a preset alarm threshold. The acquisition cost is around 1,000 euros.

· Intermediate-grade unit: A GNSS receiver striking a balance between moderate positional precision and a price point considerably lower than premium offerings. It also incorporates an integrity monitoring mechanism (though not aligned with DO-229) and generates Protection Level figures spanning horizontal and vertical axes. The acquisition cost is around 200 euros.

· Consumer-grade unit: This entry-level GNSS receiver falls into the mass-market category, targeting everyday consumer use while trading sophisticated functionality for minimal cost. Such a device generates neither Protection Level values nor any form of advanced integrity oversight of the position solution it produces. The acquisition cost stays under one hundred euros.

· TSO-certified unit: The designation applies to a GNSS receiver whose design has been approved under a Technical Standard Order (TSO) issued by regulatory agencies such as the FAA (Federal Aviation Administration) or the EASA (European Aviation Safety Agency). A TSO establishes the baseline performance benchmark for specified materials, components, and equipment installed on civil aircraft. This unit was never flown on a UAS platform; its recorded output is included solely for reference.

The results are conveyed through a tabulated statistical overview (utilizing mean values, 95th percentile thresholds, and/or peak recorded values) covering a selection of GNSS performance indicators:

· HDOP and VDOP (P95): These entries capture the Horizontal Dilution of Precision (HDOP) and Vertical Dilution of Precision (VDOP) thresholds that encompass 95% of all observations collected across the entire measurement period.

· NSV used (mean): This entry captures the typical number of GNSS space vehicles actively contributing to each position fix computation, averaged over the full observation window.

· C/N0 mean [dB-Hz]: This entry corresponds to the mean Carrier-to-Noise Density Ratio characterizing received GNSS signals, expressed using the decibels–Hertz (dB-Hz) unit.

© 2023 The Author(s). | Published by Agro Intelligence Research Press

· HPE/VPE Error [m]: Horizontal/Vertical Position Error (HPE/VPE) quantifies, in metre units, the offset separating the GNSS-derived horizontal/vertical position estimate from the independently established reference location. Tabulated entries where PE exceeds 4 m receive light red highlighting.

· HPL/VPL [m]: Horizontal/Vertical Protection Level constitutes a statistically derived bound intended to envelope the largest Horizontal/Vertical Position Error a GNSS receiver might plausibly encounter, established at an extremely high confidence threshold—the conventional figure being 99.999% (corresponding to an integrity risk of 10−5)—though certain receiver models permit user adjustment of this parameter. Such bounds are indispensable within safety-critical operating contexts, aviation foremost among them, to safeguard the trustworthiness of the position solution.

Tabulated entries where HPL climbs beyond 40 m or VPL climbs beyond 35 m (thresholds aligned with the alarm limits prescribed for LPV200 [9]) receive blue highlighting. Only within the EGNOS configuration do the computed PLs adhere to the DO-229 standard. Receiver manufacturers do not publicly document in their technical datasheets the detailed methodology used to compute PLs when operating outside the SBAS configuration.

· HPE-HPL and VPE-VPL: These quantities represent, epoch by epoch, the arithmetic difference obtained by subtracting the Protection Level value from the corresponding Position Error value. The tabulated result presents only the largest difference observed throughout the entire trial. A negative result indicates that the Protection Level envelope consistently exceeded the Position Error across all epochs, meaning zero Misleading Information events transpired—a concept elaborated upon below. A positive result discloses the magnitude by which Position Error broke through the Protection Level boundary, signifying that an MI event did occur.

· Hacc/Vacc [m]: This pair denotes the sensor's real-time estimate of horizontal and vertical accuracy. These numbers serve as upper confidence bounds for the horizontal and vertical position errors, providing a statistical assurance of at least 95%. Due to limitations imposed by the receiver's configuration options, recording these metrics was feasible only for the premium-grade unit when configured for EGNOS.

· Integrity Monitoring Alarm: For receiver models that can assert an integrity monitoring status flag, this entry tallies the number of integrity monitoring alarms logged. Analysis of the premium-grade unit revealed that the alarm assertion logic fires when either a failure to converge on a position solution or a rise in Protection Levels reaches an excessively elevated regime. For the TSO-certified unit, an SBAS-unavailable condition is declared at any moment when HPL > HAL and/or VPL > VAL, and the count of such occurrences is captured under this parameter. The TSO-certified unit's configuration employed HAL set to 40 m, and VAL set to 35 m, mirroring the specifications of the LPV200 precision approach procedure.

· MI events: A tally of Misleading Information (MI) epochs (logged at 1 Hz), identified through post-processing, representing those sampling instants where the computed Horizontal/Vertical Position Error (HPE/VPE) broke through its associated Horizontal/Vertical Protection Level (HPL/VPL) envelope. The reported figure aggregates Horizontal MIs (HPE > HPL) together with Vertical MIs (VPE > VPL). The presentation takes the form of an absolute count of such breaches, supplemented by the proportion of breach events attributable to the horizontal or vertical component, each expressed relative to the total epoch population collected during the data acquisition run.

· Est. Acc. Alarms: A tally of epochs (at 1 Hz), derived through post-processing, corresponding to sampling instants where the Horizontal/Vertical Position Error (HPE/VPE) was found to surpass the Horizontal/Vertical Estimated Error (Hacc/Vacc) bound. The reported figure sums across both horizontal (HPE > Hacc) and vertical (VPE > Vacc) alarm conditions.

Stationary testing

The current section documents the stationary testing program introduced above, along with the acquired datasets and the interpretation drawn from their examination.

© 2023 The Author(s). | Published by Agro Intelligence Research Press

Nominal scenario

The focus of this subsection falls upon the baseline performance characterisation of a premium-grade receiver deliberately configured for several distinct constellation tracking modes, alongside a comparative evaluation spanning multiple UAS-market receiver grades (a TSO-certified unit included) while all are set to SBAS tracking mode—the objective being to gauge their behaviour under entirely unobstructed sky-view conditions, absent L1-band interference, free of ionospheric disturbance, with a receiver-imposed elevation mask fixed at 5 degrees, and with no signal anomalies whatsoever. The collected metrics remain within the expected operational envelope documented for each sensor in its respective datasheet.

Premium-grade receiver operating under several distinct GNSS positioning modes

Illustrating the point, the metrics gathered using a premium-grade receiver throughout a 24-hour window on 06.05.2025 are presented, spanning the following GNSS positioning mode configurations: GPS L1 + EGNOS, GPS Standalone (L1/L2), GPS + GAL (L1/L2 + E1/E5), and Galileo alone (E1/E5). **Table 1** compiles the results obtained over the full measurement run.

Table 1. Nominal behaviour: Premium-grade receiver across several GNSS position mode configurations.

Parameter		High-end receiver			
		Galileo	**GPS + GAL**	**GPS**	**EGNOS**
HDOP (P95)		1.35	0.79	1.06	1.11
VDOP (P95)		2.67	1.22	1.59	1.64
NSV used (mean)		9.16	18.94	9.77	9.59
C/N_0 mean [dB-Hz]		39.11	38.61	40.11	40.72
HPE [m]	**Max**	2.48	2.39	3.28	0.69
	P95	2.35	1.87	2.1	0.45
	Mean	1.2	0.79	0.93	0.24
HPL [m]	**Max**	47.57	19.98	29.53	13.38
HPE-HPL [m]	**Max**	−45.09	−17.59	−26.25	−12.69
Hacc [m]	**Max**	18.56	5.64	6.93	3.33
	P95	15.74	5.19	6.52	2.67
	Mean	10.69	4.95	6.05	2.23
Hacc–HPE [m]	**Max**	16.08	3.25	3.65	2.64
VPE [m]	**Max**	2.55	4.07	4.69	1.17
	P95	2.05	4.01	4.42	0.87
	Mean	0.94	2.14	2.13	0.32
VPL [m]	**Max**	68.84	33.08	44.22	21.58
VPE-VPL [m]	**Max**	−66.79	−29.07	−39.53	−20.41
Vacc [m]	**Max**	28.88	8.59	15.77	4.67

© 2023 The Author(s). | Published by Agro Intelligence Research Press

	P95	22.35	7.79	10.64	3.57
	Mean	15.39	7.08	8.6	3.02
Int. Monitoring Alarm		N/A	N/A	N/A	0
MI events		0	0	0	0
Est. Acc. Alarms		N/A	N/A	N/A	0

Seeing as the scenario introduces no anomaly of any description, the Position Errors remained within their nominal bounds, and the receiver logged no integrity monitoring alarm activations. What is more, no MI events occurred, just as zero Est. Acc. Alarms were recorded. The Protection Level values generated during Galileo tracking exhibited pronounced variability, occasionally spiking to magnitudes far removed from the concurrently observed Position Error values. Inspection of the table reveals that the estimated accuracy values are lower than the computed PLs.

Several UAS-market receiver grades configured for SBAS tracking

A representative sample of the nominal performance over 24 hours on 06.05.2025 by a premium-grade unit, an intermediate-grade unit, a consumer-grade unit, and a TSO-certified aviation unit—all configured to track SBAS—is presented. **Table 2** compiles the results gathered from each distinct receiver grade over the full measurement run.

Table 2. Nominal behaviour (EGNOS): Several receiver grades.

Parameter		**EGNOS**			
		TSO	**Low-End**	**Mid-Range**	**High-End**
HDOP (P95)		1.44	1.09	1.1	1.11
VDOP (P95)		1.62	1.62	1.63	1.66
NSV used (mean)		9.65	9.71	9.67	9.59
C/N_0 mean [dB-Hz]		36.32	44.72	44.54	40.72
HPE [m]	**Max**	1.72	2.41	2.45	0.69
	P95	1.04	1.19	1.56	0.45
	Mean	0.51	0.58	1.06	0.24
HPL [m]	**Max**	14.47	N/A	6.81 *	13.38
HPE-HPL [m]	**Max**	−12.75	N/A	−4.36	−12.29
VPE [m]	**Max**	3.7	5.42	3.82	1.17
	P95	2.25	2.02	1.72	0.87
	Mean	0.98	0.83	0.79	0.32
VPL [m]	**Max**	26.29	N/A	5.78 *	21.58
VPE-VPL [m]	**Max**	−22–59	N/A	−1.96	−20.41
Int. Monitoring Alarm		0	N/A	N/A	0
MI events		0	N/A	0	0

* The PL figures displayed for this receiver were not derived according to the methodology prescribed by DO-229.

© 2023 The Author(s). | Published by Agro Intelligence Research Press

To synthesise the above: under nominal operating conditions devoid of degradation sources, the GNSS positioning output remains both precise and dependable, in harmony with the specifications published for each receiver. Turning to those units equipped with integrity monitoring that supply Protection Levels computed in accordance with DO-229, as indicated by their respective specification sheets, the Position Errors are observed to reside inside the envelope bounded by the corresponding Protection Levels in both the horizontal and vertical planes for the entire measurement duration, with a comfortable safety margin. For the intermediate-grade unit whose design does not implement DO-229, the Protection Levels remain larger than the Position Errors they envelop. Still, the safety margin is notably thinner than that maintained by the premium-grade PLs.

Ionospheric disturbance scenario

With a view toward appreciating the extent to which ionospheric disruptions can undercut the accuracy of GNSS-derived positions, a dedicated measurement campaign was timed to coincide with a period of pronounced ionospheric unrest. For the duration of this test, the antenna sat beneath wide-open skies, encountering neither signal obscuration nor L1-band emissions. The ionospheric event targeted for scrutiny unfolded on 14 February 2025. Over the course of that day, the Kp index surpassed 3 on multiple occasions. **Table 3** summarises the collected data.

Table 3. Ionospheric disturbance scenario (EGNOS): Assorted receiver categories.

Parameter		EGNOS			
		TSO	Low-End	Mid-Range	High-End
HDOP (P95)		1.31	1.09	1.09	1.32
VDOP (P95)		1.84	1.78	1.77	2.60
NSV used (mean)		9.4	9.72	9.73	9.33
C/N_0 mean [dB-Hz]		36.19	45.16	44.38	40.76
HPE [m]	Max	2.69 [1]	5.98	6.56	0.74 [1]
	P95	1.25 [1]	1.83	3.18	0.54 [1]
	Mean	0.55 [1]	0.77	1.53	0.25 [1]
HPL [m]	Max	47.25	N/A	13.26 *	51.31
HPE-HPL [m]	Max	−44.56	N/A	1.39	−5.75
Hacc [m]	Max	N/A	N/A	N/A	11.4
	P95	N/A	N/A	N/A	5.1
	Mean	N/A	N/A	N/A	2.9
VPE [m]	Max	3.48 [1]	5.92	10.42	1.05 [1]
	P95	1.51 [1]	2.52	5.18	0.83 [1]
	Mean	0.61 [1]	1.06	1.42	0.36 [1]
VPL [m]	Max	37.91	N/A	11.03 *	38.61
VPE-VPL [m]	Max	−7.10	N/A	6.35	−8.53
Vacc [m]	Max	N/A	N/A	N/A	9.42
	P95	N/A	N/A	N/A	5.55

© 2023 The Author(s). | Published by Agro Intelligence Research Press

Mean	N/A	N/A	N/A	3.61
Int. Monitoring Alarm	1084	N/A	N/A	0
MI events [number] (H/V %)	0	N/A	8052 0.74/8.58	0
Est. Acc. Alarms	N/A	N/A	N/A	0

* These PLs were generated without adherence to the DO-229 methodology. 1 Omitting epochs wherein the receiver could no longer sustain an LPV200-grade service, defined by HPL > 40 m or VPL > 35 m.

Units that derive Protection Levels consistent with the RTCA DO-229 framework (specifically the premium-grade receiver and the TSO-certified unit) registered numerous epochs whose Position Errors bore the imprint of the ionospheric event, climbing to worst-case Horizontal Position Error figures of 0.74 m and 2.69 m, respectively. The Protection Levels emitted by both receivers swelled markedly in response **(Figure 1)**. On each device, the operator was both notified and shielded at times when the GNSS position fix became compromised **(Figure 2)**. The SBAS architecture performs continuous ionospheric surveillance, and the resulting Protection Levels serve to bound the position estimate against unsafe errors whenever ionospheric activity intensifies.

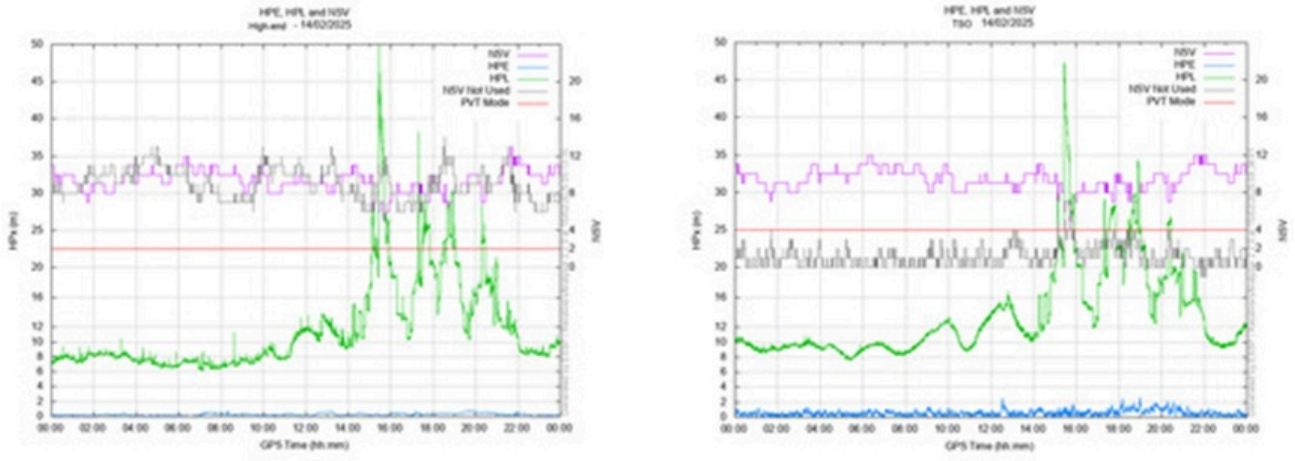

Figure 1. Premium-grade and TSO-certified receivers: HPE, HPL, and satellite population against time.

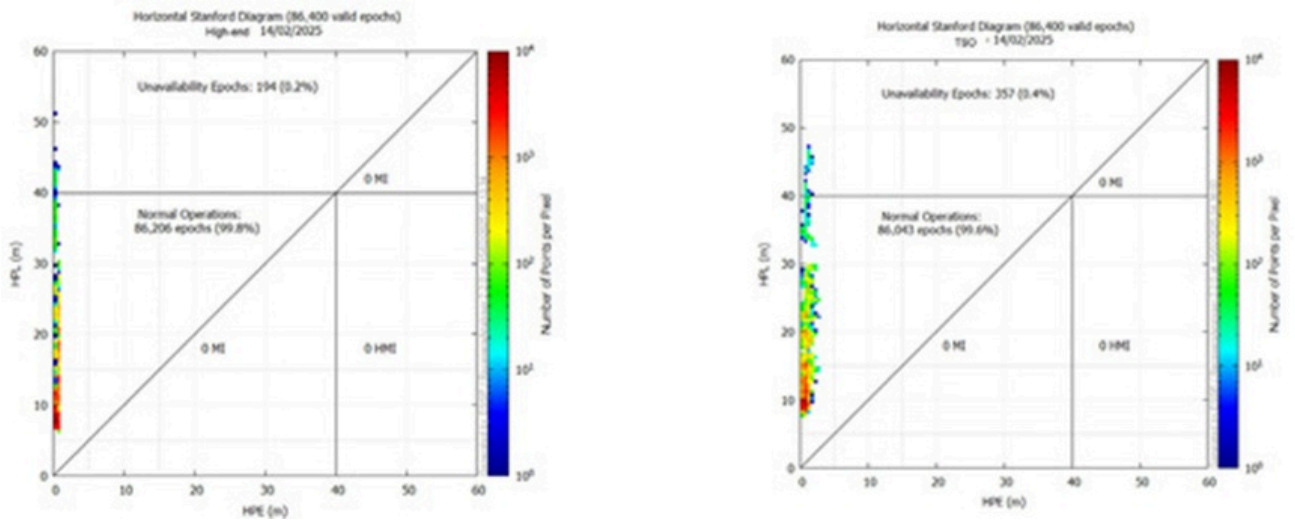

Figure 2. Premium-grade and TSO-certified receivers: Horizontal Stanford Diagram.

© 2023 The Author(s). | Published by Agro Intelligence Research Press

Also apparent from **Table 3** is that the estimated accuracy stream produced by the premium-grade receiver maintained values exceeding the positioning error (Hacc > HPE and Vacc > VPE) throughout the entire logging window, resulting in no estimated accuracy alarm triggers.

By contrast, the intermediate-grade unit—whose Protection Levels do not follow the DO-229 prescription—returned values that did not inflate enough to reliably cap the Position Errors set off by the ionospheric disturbance. The outcome was 638 Horizontal MI events (epochs where HPE > HPL) and 7414 Vertical MI events (epochs where VPE > VPL), aggregating to 8052. Throughout the window of heightened error, Vertical Position Error reached a peak of 10.4 m. At the same time, the observed satellite tally and Dilution of Precision metrics shifted only modestly relative to the nominal reference day (both HDOP and VDOP peaked at 1.3). Nevertheless, the Horizontal Position Error effectively doubled, even though it failed to trigger any operator alert on those receivers that do not incorporate SBAS-based standard residual error models into their Protection Level computation.

Multipath scenario

In this instance, the receivers occupied a fixed metropolitan position, placed such that a neighbouring high-rise building masked a substantial fraction of the visible sky hemisphere. Direct lines of sight to the complete GNSS constellation were therefore unavailable, and the antenna collected a rich mixture of reflected multipath signals. Data were collected continuously over 24 hours on 26 March 2025, characterising behaviour under GPS Standalone (L1/L2), GPS + GAL (L1/L2 + E1/E5), and Galileo-only (E1/E5) tracking modes, utilising both premium-grade and intermediate-grade devices.

Starved of adequate satellite visibility, Position Error magnitudes expanded beyond the nominal benchmark in both horizontal and vertical axes. Scanning the various receiver configurations, the premium-grade unit registered 4326 alarm activations traceable to elevated Protection Levels, thereby alerting the user that the GNSS position had deteriorated. The intermediate-grade device—whose Protection Levels do not conform to DO-229—generated PL values that did not contain the corresponding Position Errors across every epoch. Post-processing confirms 413 distinct epochs during which either HPE > HPL or VPE > VPL occurred.

As reflected in **Table 4**, the average satellite count utilised contracted across all positioning modes (for example, under EGNOS, the figure dropped from 9.28 in the nominal scenario to 7.13), and both HDOP and VDOP rose (EGNOS HDOP moved from 1.08 in the nominal scenario to 2.83). Yet neither deterioration was severe enough to trigger a user alert independently. Moreover, C/N0 levels showed a degrading influence from multipath, with depressed values, though distinguishing whether a given correlation peak belongs to the direct path or a reflection is far from trivial. The dataset clearly indicates that the receiving antenna was located at a site where a tall structure northwest of its position interrupted the direct propagation path, as illustrated in **Figure 3** by comparison with a concurrently operating open-sky reference antenna. The upper panels of each scenario plot depict per-satellite signal quality—rendered as Signal-to-Noise Ratio (SNR)—which is markedly poorer in the multipath-affected setting than in the open-sky case. The lower panels, for their part, plot the pseudorange residual errors for each satellite; under multipath conditions, these residuals grow, in some instances culminating in the complete dropout of signals from satellites masked toward the northwest.

© 2023 The Author(s). | Published by Agro Intelligence Research Press

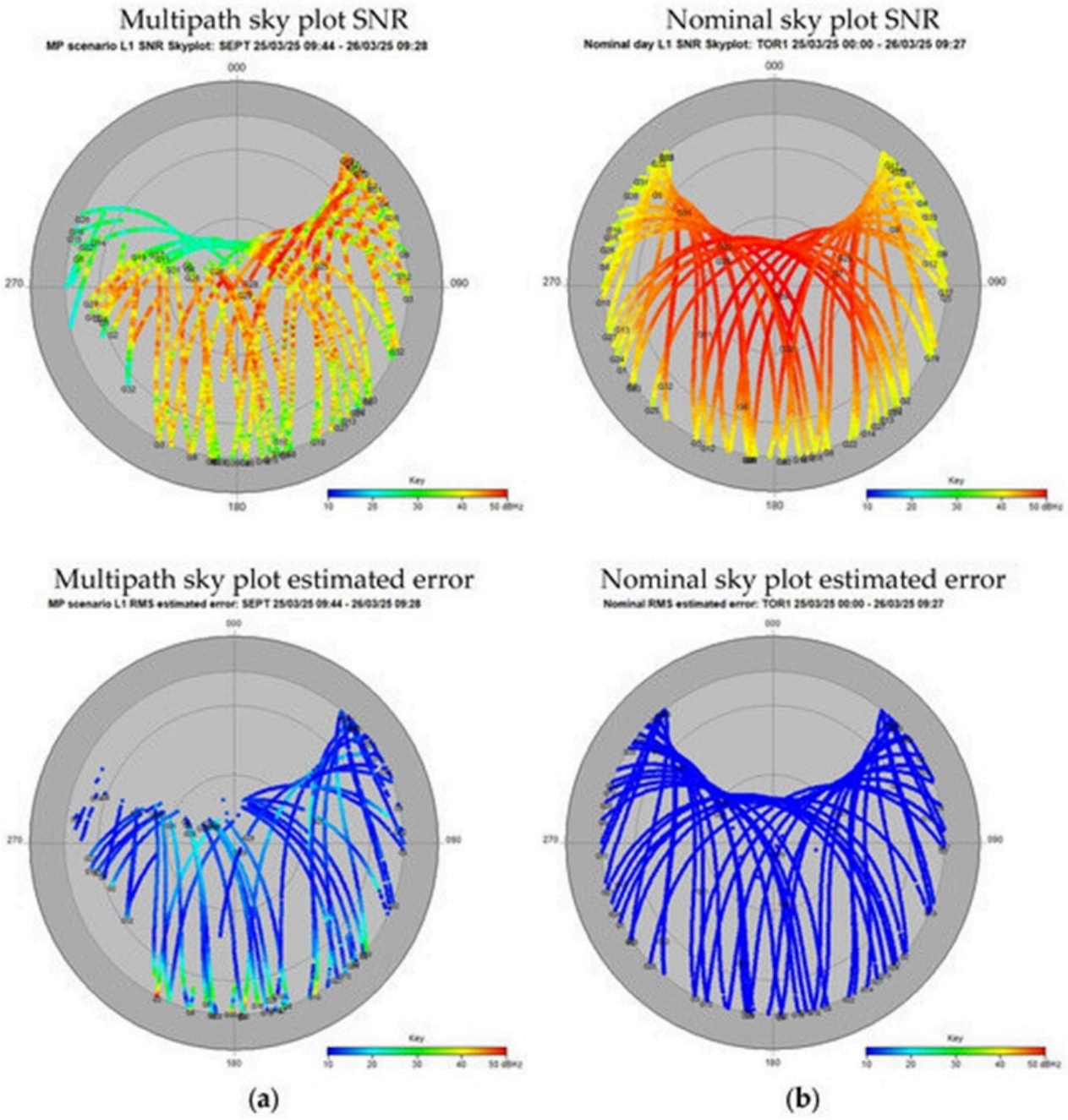

Figure 3. Sky plot: (a) Multipath-affected setting, and (b) Open-sky setting.

Table 4. Multipath scenario. A premium-grade receiver across several GNSS position modes, together with an intermediate-grade receiver using EGNOS.

Parameter	Mid-Range PL	High-end receiver			
	EGNOS	Galileo	GPS + GAL	GPS	EGNOS
HDOP (P95)	1.51	2.41	1.20	2.77	2.83
VDOP (P95)	6.94	19.03	1.97	69.84	10.47

© 2023 The Author(s). | Published by Agro Intelligence Research Press

NSV used (mean)		11.69	7.44	14.53	7.35	7.13
C/N_0 mean [dB-Hz]		41.85	38.34	39.04	39.74	40.80
HPE [m]	**Max**	18.76	13.13	4.87	6.91	4.75 [1]
	P95	7.22	6.18	3.71	4.57	3.33 [1]
	Mean	3.28	3.04	1.88	2.18	2.41 [1]
HPL [m]	**Max**	762.94 *	611.75 *	52.04 *	848.34 *	1000
HPE-HPL [m]	**Max**	2.61	−598.62	−47.17	−841.43	−995.25
Hacc [m]	**Max**	2.19	167.84	14.22	152.76	144.99
	P95	1.26	29.63	9.88	19.39	8.27
	Mean	0.86	16.39	6.86	10.38	5.6
Hacc-HPE [m]	**Max**	−16.75	154.71	9.35	145.85	449.25
VPE [m]	**Max**	31.2	10.6	3.19	11.83	7 [1]
	P95	10.94	5.07	2.89	4.91	6.6 [1]
	Mean	4.96	2.34	1.78	2.37	4.45 [1]
VPL [m]	**Max**	1010.66 *	215.92 *	92.83 *	663.31 *	1687.34
VPE-VPL [m]	**Max**	7.35	−205.32	−89.64	−651.48	−1680.34
Vacc [m]	**Max**	3.43	163.67	26.13	152.75	130.57
	P95	1.67	54.22	14.5	21.59	8.63
	Mean	1.09	23.97	9.66	13.86	7.1
Vacc-VPE [m]	**Max**	−27.69	153.07	22.94	140.92	123.57
Int. Monitoring Alarm		Proprietary	N/A	N/A	N/A	4326
MI events [number] (H/V %)		413 (0.01/0.88)	0	0	0	0

* These PLs were generated without adherence to the DO-229 methodology. 1 Omitting epochs wherein an integrity monitoring alarm was actively asserted.

Interpreting this scenario, the SBAS-enabled receiver that produces DO-229-conformant Protection Levels raised integrity alarms at times when multipath corrupted its measurements, coinciding with enlarged Position Errors **(Figure 4)**. The intermediate-grade device returned Protection Levels that did not comply with DO-229 and were unable to bound Position Errors across the entire data record; 413 epochs exist in which horizontal or vertical error components penetrated their respective PL envelopes (as determined during post-processing scrutiny). One should additionally underscore that between approximately epoch 2.5×10^4 and epoch 3×10^4 in **Figure 4**, the HPL magnitude moves past the 50 m vertical plotting limit and is accordingly absent from the displayed range.

© 2023 The Author(s). | Published by Agro Intelligence Research Press

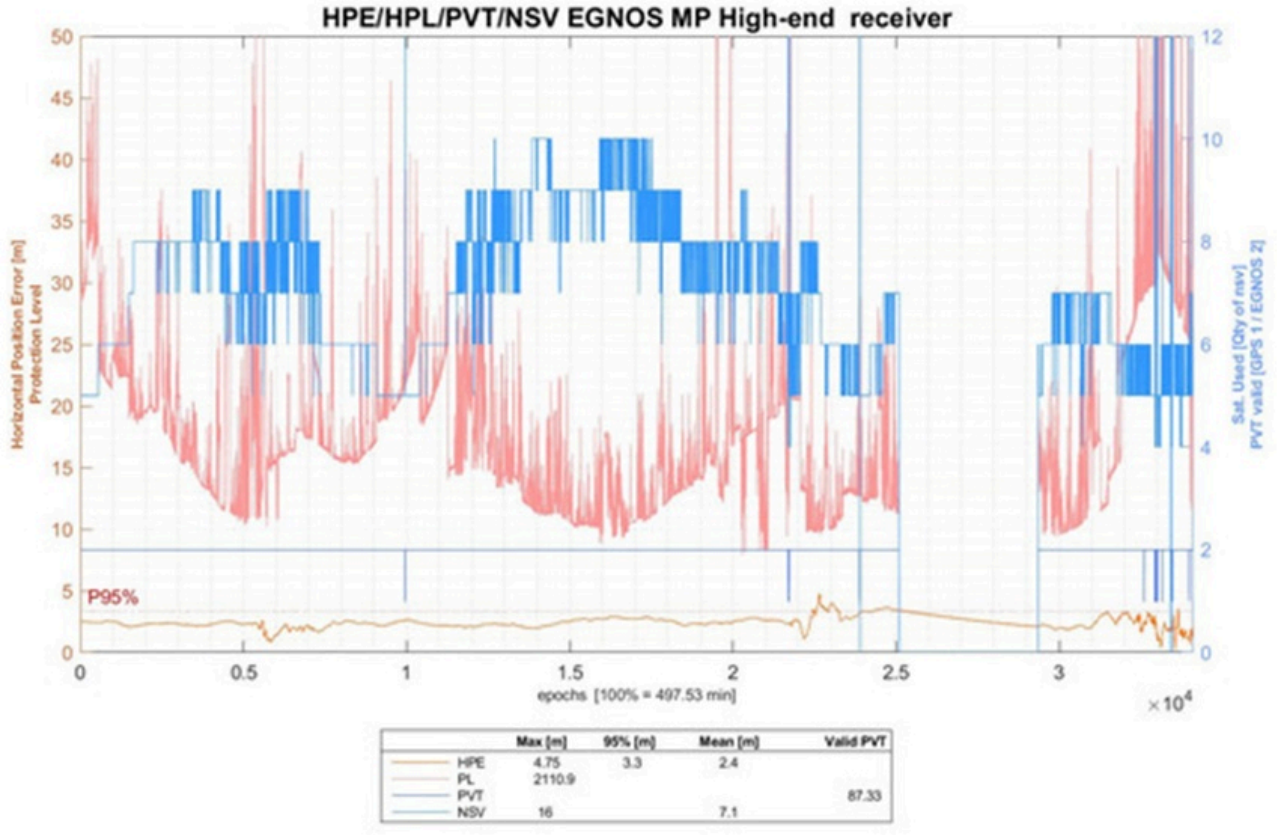

Figure 4. Premium-grade receiver tracking EGNOS in a multipath scenario.

Considering the estimated accuracy indicators (Hacc/Vacc) presented in **Table 4**, a total of 14,405 epochs (at 1 Hz) can be found where Position Error overtakes the estimated accuracy bound (HPE > Hacc or VPE > Vacc), a circumstance visualised in **Figure 5**. In the preponderance of these epochs, the vertical component is responsible for the exceedance. As anticipated, the estimated accuracy value lies below the HPL value.

© 2023 The Author(s). | Published by Agro Intelligence Research Press

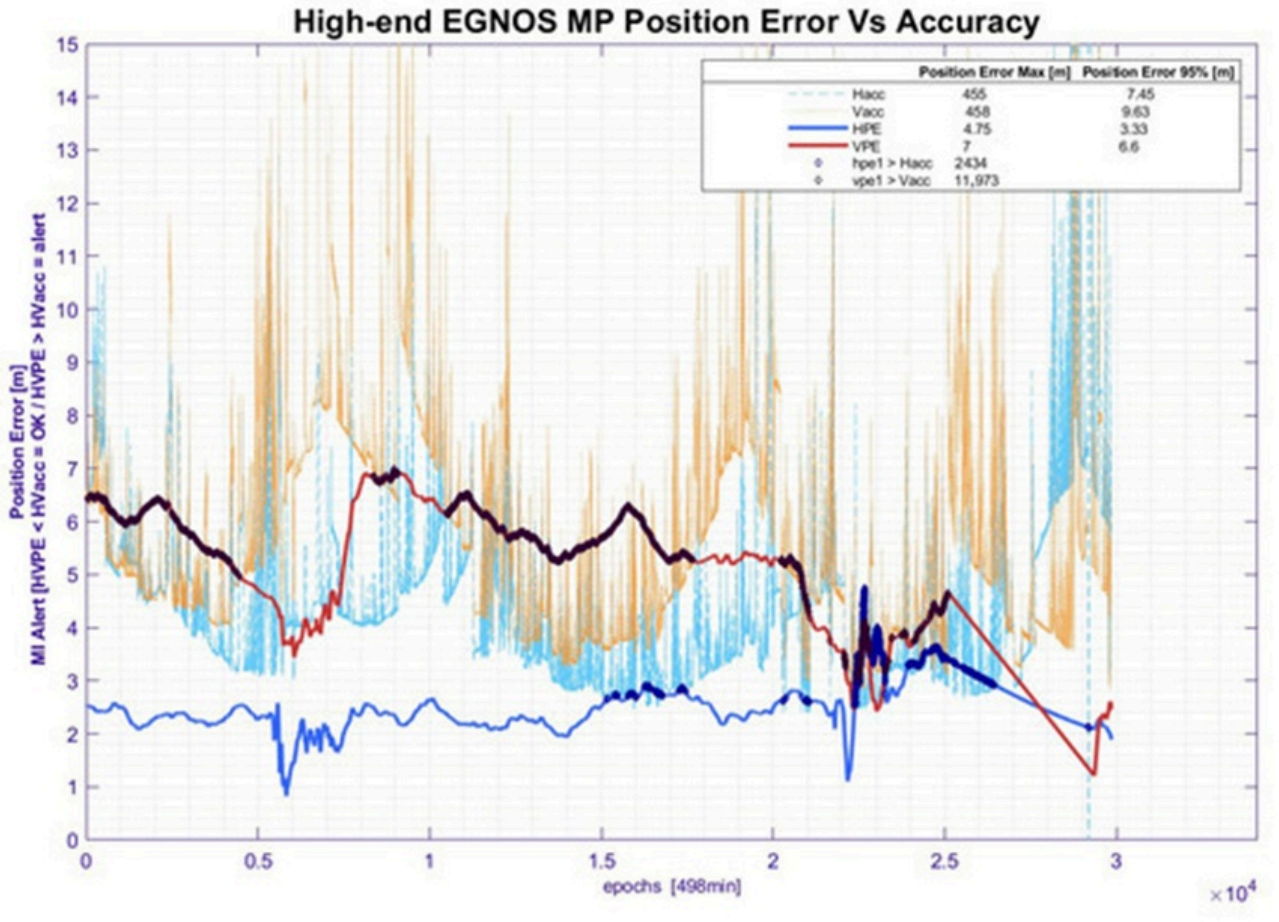

Figure 5. Premium-grade receiver. Estimated accuracy plotted against position error.

Combined multipath and ionospheric disturbance scenario

While the multipath data collection detailed above was ongoing, an ionospheric disturbance manifested on 25.03.25, and its signature was captured using a premium-grade receiver arranged for GPS Standalone (L1/L2), GPS + GAL (L1/L2 + E1/E5), and Galileo (E1/E5), alongside an intermediate-grade unit restricted to EGNOS only. **Table 5** displays the findings.

Table 5. Combined multipath and ionospheric disturbance scenario: Premium-grade receiver under assorted configurations, together with an intermediate-grade receiver using EGNOS.

Parameter		Mid-Range	High-End Receiver			
		EGNOS	Galileo	GPS + GAL	GPS	EGNOS
HDOP (P95)		1.4	3.14	1.35	2.51	3.09
VDOP (P95)		2.08	4.7	1.75	3.09	3.65
NSV used (mean)		13.81	6.64	13.63	7.12	6.78
C/N_0 mean [dB-Hz]		34.80	37.61	38.22	38.83	28.62
HPE [m]	Max	18.76	91.06	12.57	57.86	105.47 [1]
	P95	6.88	8.64	3.89	19.71	3.6 [1]

© 2023 The Author(s). | Published by Agro Intelligence Research Press

	Mean	3.25	3.39	1.81	4.07	2.84 [1]
HPL [m]	**Max**	762.94 *	1000 *	58.21 *	1176 *	1000
HPE-HPL [m]	**Max**	3.65	−908.94	−45.64	−1118.14	−894.53
Hacc [m]	**Max**	2.79	180.43	15.34	190.96	149
	P95	1.33	42.12	10.9	21.23	9.9
	Mean	0.85	18.24	7.76	12.03	6.24
Hacc-HPE [m]	**Max**	15.97	89.37	2.77	133.10	43.53
VPE [m]	**Max**	31.2	10.6	3.19	11.83	134 [1]
	P95	10.94	5.07	2.89	4.91	6.6 [1]
	Mean	4.96	2.34	1.78	2.37	4.82 [1]
VPL [m]	**Max**	1010.66 *	215.92 *	92.83 *	663.31 *	1687.34
VPE-VPL [m]	**Max**	10.87	−205.32	−89.64	−651.48	−1553.34
Vacc [m]	**Max**	5.31	361.27	29.6	175.51	190
	P95	1.69	58.29	14.68	33.02	13.1
	Mean	1.03	26.79	10.82	17.52	8.46
Vacc-VPE [m]	**Max**	−25.89	350.67	26.41	163.68	56
Int. Monitoring Alarm		Proprietary	N/A	N/A	N/A	1193
MI events [number] (H/V %)		1103 (0.02/2.22)	0	0	877 (0/1.76)	0

* These PLs were generated without adherence to the DO-229 methodology. 1 Omitting epochs wherein an integrity monitoring alarm was actively asserted.

The juxtaposition of multipath reflections and ionospheric disturbance constitutes one of the most unforgiving operational backdrops any GNSS receiver—whether single- or multi-constellation—can confront. The collected evidence shows both devices reacting with heightened Protection Levels and enlarged Position Errors in the face of this combination. The premium-grade unit logged 1193 integrity alarms while operating on the SBAS solution **(Figure 6)**, successfully delivering a warning to the operator **(Table 5)**. Indeed, the receiver autonomously abandoned the EGNOS fix in favour of standalone GPS at junctures where computing a trustworthy SBAS position became impossible. Even so, the GPS and Galileo configurations experienced several MI events. The intermediate-grade PL receiver accumulated 1103 MIs, its Protection Levels (whose derivation lies outside DO-229) proving insufficient to bound the observed Position Errors.

© 2023 The Author(s). | Published by Agro Intelligence Research Press

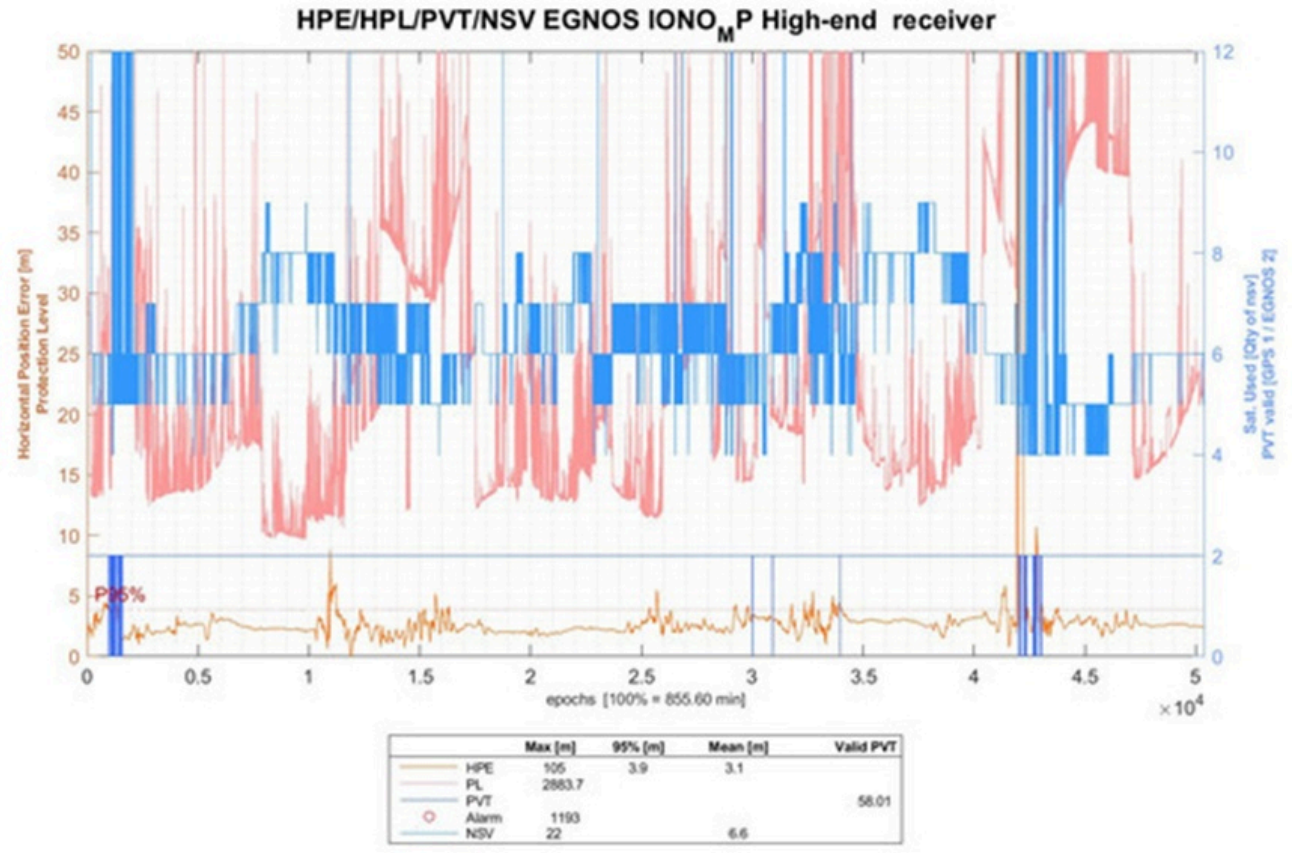

Figure 6. Premium-grade receiver tracking EGNOS; combined multipath and ionospheric disturbance scenario.

L1 Interference scenario

This scenario documents the data recorded throughout an L1-band interference incident that occurred on 22.09.2024 **(Table 6)**. The measurements were logged by the complete suite of GNSS receivers introduced in Section 3, uniformly configured to track EGNOS.

Table 6. L1 interference scenario (EGNOS) spanning assorted receiver types.

Parameter		EGNOS			
		TSO	Low-end	Mid-range	High-end
HDOP (P95)		1.19	1.1	1.1	1.21
VDOP (P95)		1.78	1.72	1.72	1.76
NSV used (mean)		9.57	9.73	9.73	9.78
C/N_0 mean [dB-Hz]		42.88	45.30	45.25	40.66
HPE [m]	Max	4.78	2.44	3.47	4.43 [1]
	P95	1.01	1.23	1.71	0.81 [1]
	Mean	0.50	0.61	1.03	0.44 [1]
HPL [m]	Max	832	N/A	7.57 *	1000

© 2023 The Author(s). | Published by Agro Intelligence Research Press

HPE-HPL [m]	**Max**	−827.22	N/A	−4.1	−995.47
VPE [m]	**Max**	8.42	4.12	3.92	9.94 [1]
	P95	2.13	1.92	2.02	1.21 [1]
	Mean	0.87	0.81	0.86	0.52 [1]
VPL [m]	**Max**	189	N/A	6.51 *	1000
VPE-VPL [m]	**Max**	−180.6	N/A	0.42	−990.06
Int. Monitoring Alarm		2051	N/A	Proprietary	369
MI events [number] (H/V %)		0	N/A	46 (0/0.05)	0

* These PLs were generated without adherence to the DO-229 methodology. 1 Omitting epochs wherein an integrity monitoring alarm was actively asserted.

Scrutiny of the L1-band jamming event shows the premium-grade unit issuing 369 integrity monitoring alarm assertions **(Figure 7)**. At the same time, the intermediate-grade device recorded 46 MI epochs due to PE > PL (not aligned with DO-229). For the premium-grade unit, Protection Levels ballooned by roughly 1000 m, and a span of 369 seconds (epochs) elapsed during which the operator received explicit caution that the position solution had become untrustworthy. The TSO-certified device had been set up for LPV200 operation (with the integrity monitoring alarm firing upon HPL > 40 m or VPL > 35 m). As a result, the number of epochs during which the TSO unit declared the SBAS solution unfit for LPV200 service was considerably larger, totaling 2051 epochs (seconds).

© 2023 The Author(s). | Published by Agro Intelligence Research Press

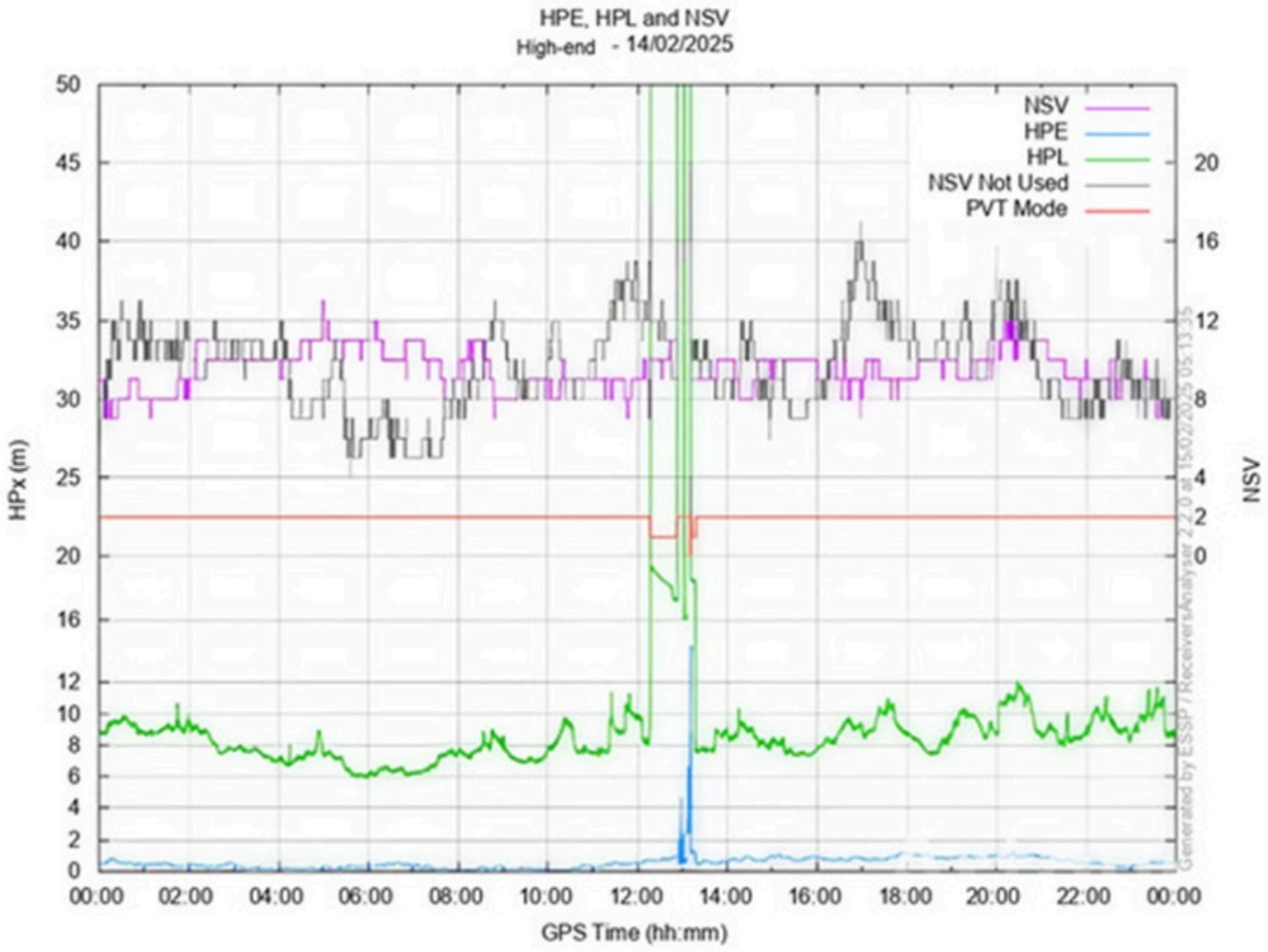

Figure 7. Behaviour of the premium-grade receiver throughout the L1 interference event.

To distil the observations, the evidence supports the conclusion that SBAS-equipped receivers whose Protection Level computation adheres to DO-229 are capable of notifying operators at times when the SBAS position fix degrades **(Figure 8)**, whether that degradation manifests as unacceptably large Position Errors or as a complete inability to calculate a GNSS fix. Protection Levels serve a valuable function by asserting both horizontal and vertical alerts whenever the receiver contends with ionospheric disturbances, signal masking, multipath reflections, or comparable phenomena, giving the UAS—and through it either the autonomous flight logic or the remote pilot—the prompt needed to enact predefined contingency flight responses tailored to such circumstances.

© 2023 The Author(s). | Published by Agro Intelligence Research Press

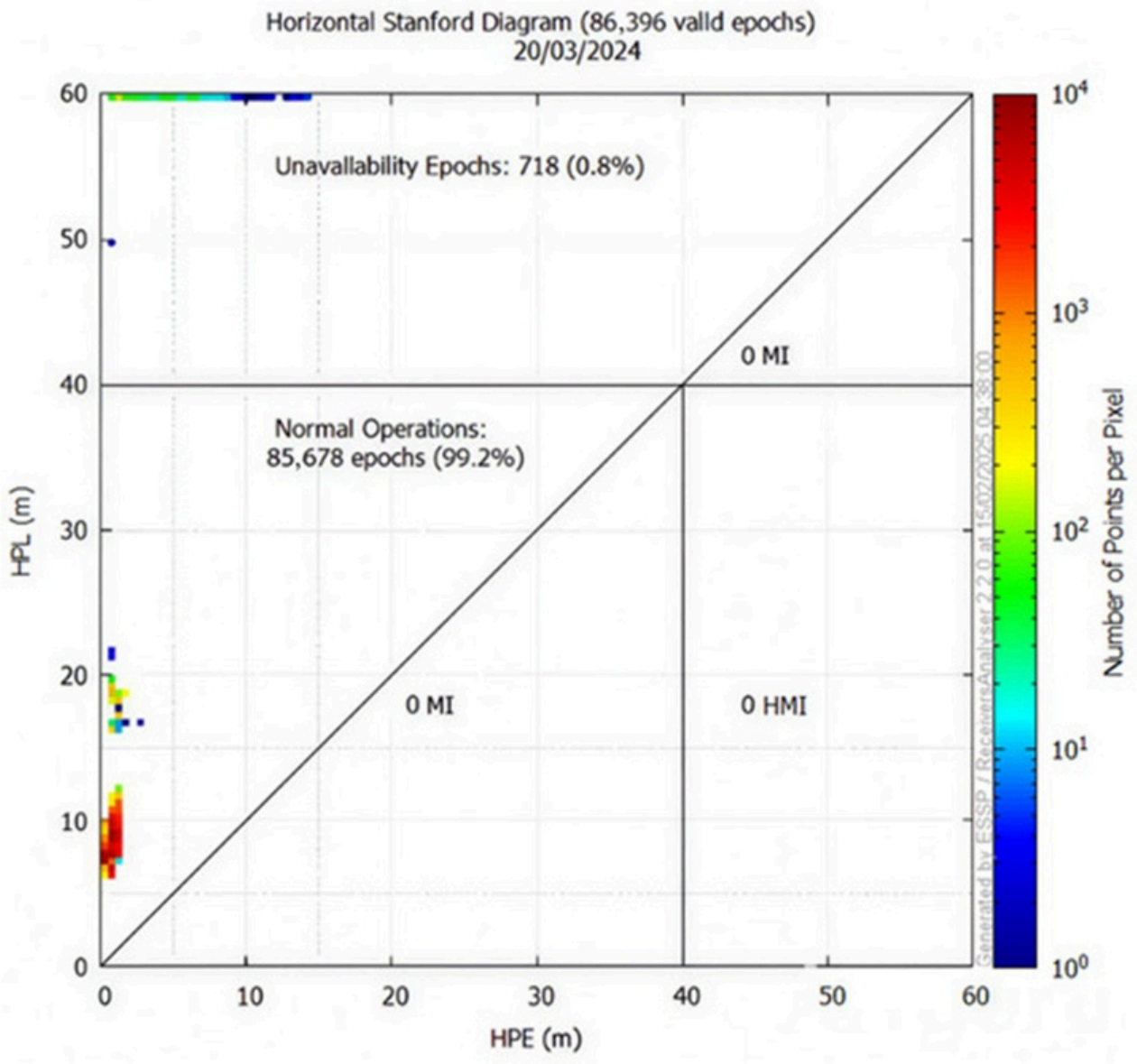

Figure 8. Horizontal Stanford Diagram for the premium-grade receiver during the L1 interference event.

UAS dynamic testing

The present subsection describes two separate experiments undertaken with sensors mounted aboard an airborne UAS. The key motivation for these experiments is to reveal how the UAS's changing orientation in flight influences GNSS measurement quality. Two distinct experiments were conducted: the first employs a routine, orderly grid flight profile, widely used for photogrammetric survey work, whereas the second pursues an intentionally erratic flight profile, in which the aircraft attitude shifts dramatically over the course of the flight. Both experiments employed a multirotor UAS airframe.

Smooth flight

This experiment was flown with an EH-1 hexacopter that executed a simple grid-based route plan **(Figure 9a)** under fully autonomous control on the 28th of November 2024 in Pozuelo del Rey, Madrid (Spain). The operation was carried out within the open category in conformity with European regulatory provisions. To be specific, the flight fell under the A3 sub-category, conducted far from uninvolved persons and at a remove from residential, commercial, industrial, and recreational precincts. This sub-category is intended for unmanned aircraft whose mass remains under 25 kg, for which

© 2023 The Author(s). | Published by Agro Intelligence Research Press

the operator is responsible for maintaining a minimum separation of 150 m from densely populated areas and for avoiding overflight of uninvolved people.

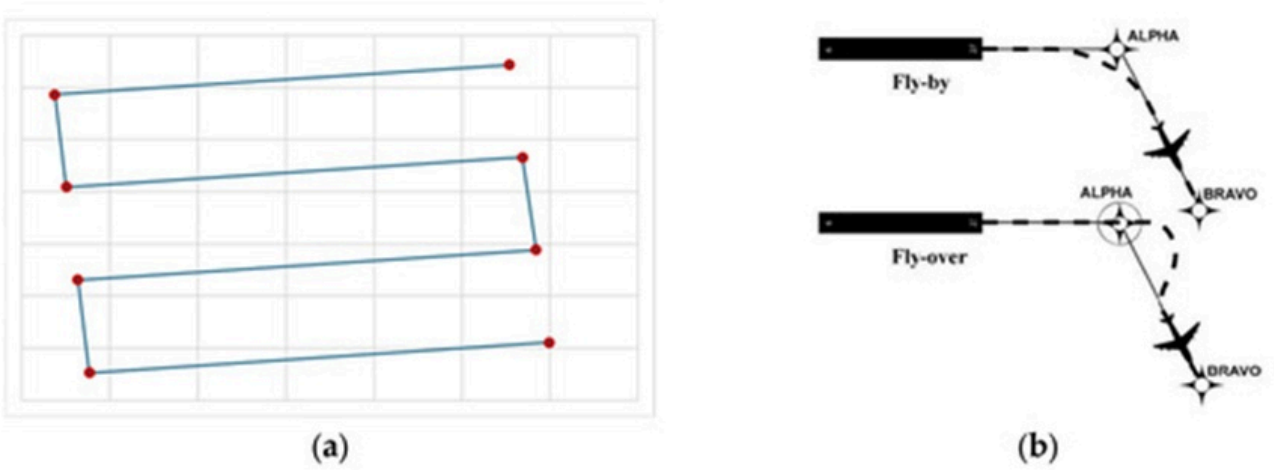

Figure 9. Smooth flight: (a) Flight trajectory, and (b) Fly-by and fly-over distinction.

The ambient environment featured a completely unobstructed sky, no interference, and no ionospheric perturbations, with the antenna mask angle set to 0°. A 4-minute flight was repeated 6 times, each tracing the trajectory shown in **Figure 9**, with the airframe consistently oriented nose-forward; the flight controller was set to fly-by (rather than fly-over) mode. All turns were conducted gently, keeping bank angles modest enough that GNSS satellite signal reception remained unimpeded. Finally, **Figure 10** provides a comparative visualisation of a single flight across the various GNSS configuration modes. For this experiment, the reference truth was supplied by a PPK solution computed in post-processing.

© 2023 The Author(s). | Published by Agro Intelligence Research Press

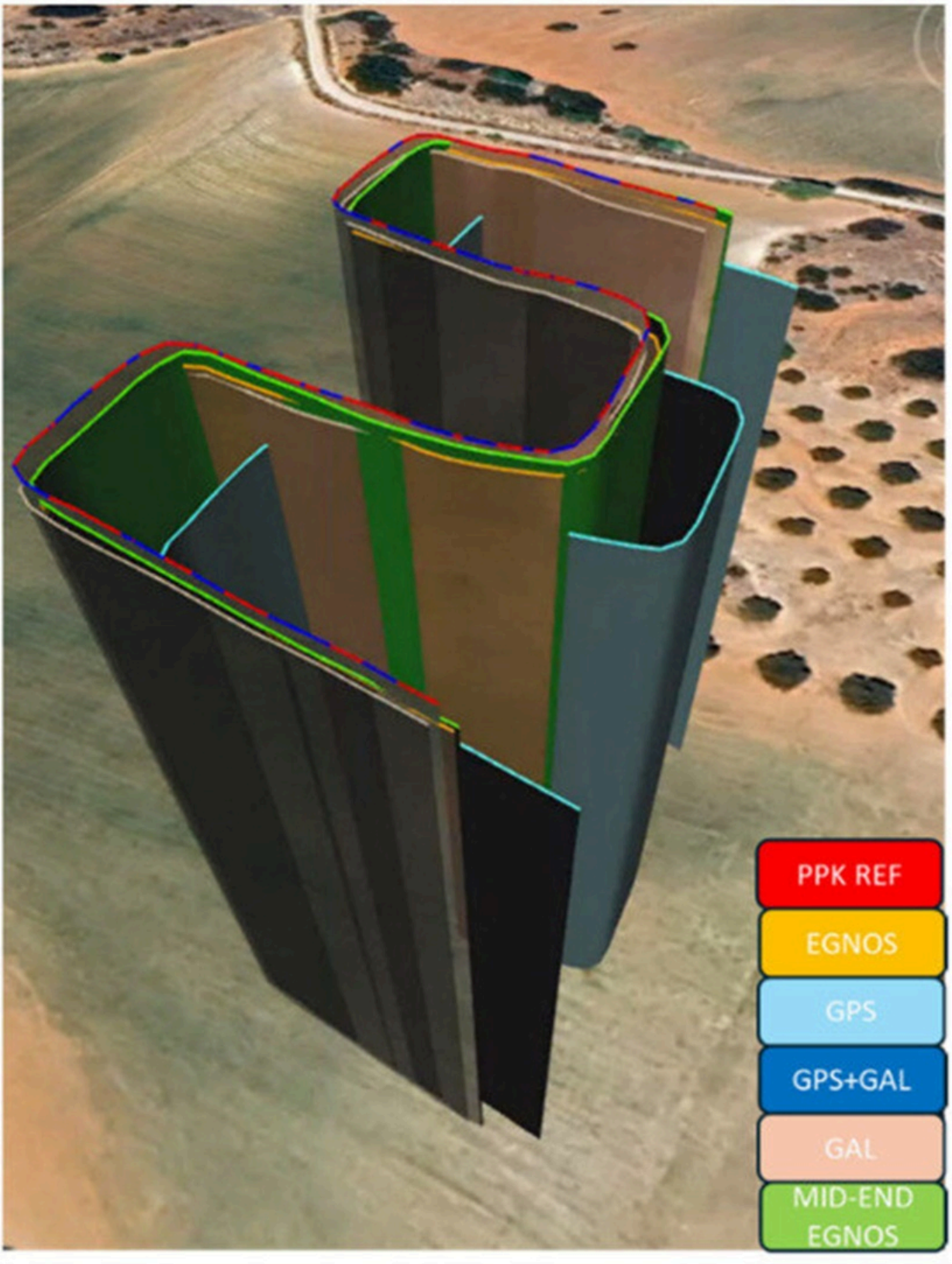

Figure 10. Three-dimensional behaviour of the premium-grade receiver under assorted GNSS positioning modes, together with the intermediate-grade receiver set to EGNOS.

© 2023 The Author(s). | Published by Agro Intelligence Research Press

The flight analysis tabulated in **Table 7** yields values consistent with nominal expectations for an open-sky sortie free from any form of disturbance or signal blockage. The EGNOS results exhibit HDOP/VDOP-P95 values below 1, while HPE/VPE-P95 are 1 m and 1.40 m, respectively. No MI events and no Integrity alarm assertions were registered. Under the conditions specific to this experiment, the recorded metrics were not corrupted by aggressive antenna attitude changes or high-speed banking manoeuvres—dynamic effects that could otherwise alter the effective mask angle and stress the receiver's high-rate signal processing chain.

Table 7. Smooth flight experiment. Premium-grade receiver under assorted GNSS position modes, together with an intermediate-grade receiver set to EGNOS.

Parameter		Mid-range	High-end receiver			
		EGNOS	Galileo	GPS + GAL	GPS	EGNOS
HDOP (P95)		0.7	1.52	0.7	0.92	0.91
VDOP (P95)		0.92	2.13	0.92	1.34	1.28
NSV used (mean)		15	6	15	9.5	9
C/N_0 mean [dB-Hz]		33.05	42.20	42.18	42.15	45.02
HPE [m]	**Max**	1.61	1.38	0.65	1.35	1.13
	P95	1.5	1.26	0.76	1.19	1.08
	Mean	1.12	0.75	0.68	1.02	0.82
HPL [m]	**Max**	3.91 *	24.45 *	7.08 *	7.86 *	16.53
HPE-HPL [m]	**Max**	−2.3	−23.07	−6.43	−6.51	−15.4
Hacc [m]	**Max**	0.82	12.26	5.33	6.96	12.26
	P95	0.53	12.24	2.59	6.78	12.24
	Mean	0.43	11.94	2.37	6.56	11.94
Hacc-HPE [m]	**Max**	0.79	8.58	4.68	0.07	11.13
VPE [m]	**Max**	1.21	1.77	0.07	1.62	1.45
	P95	1.11	1.7	0.07	1.59	1.40
	Mean	0.47	1.26	0.02	1.45	1.14
VPL[m]	**Max**	2.98 *	36.74 *	11.28 *	12.95 *	16.92
VPE-VPL [m]	**Max**	−1.77	−34.97	−11.21	−11.33	−15.47
Vacc [m]	**Max**	0.73	14.3	6.5	8.79	12.2
	P95	0.67	11.43	3.67	8.5	12.05
	Mean	0.57	9.89	3.26	7.74	3.33
Vacc-VPE [m]	**Max**	0.48	12.53	6.43	7.17	10.75
Int. Monitoring Alarm		N/A	0	0	0	0
MI events		0	0	0	0	0

© 2023 The Author(s). | Published by Agro Intelligence Research Press

* These PLs were generated without adherence to the DO-229 methodology.

Flight with high dynamics

For this experiment, the platform selected was a DJI-350 quadcopter, operated in manual flight mode **(Figure 11)** on the 7th of August 2024 in Bohadilla del Monte, Madrid (Spain). The flight adhered to the open category framework set forth by European regulations. More specifically, the sortie was conducted within the bounds of the A3 sub-category, well separated from uninvolved members of the public and at a distance from residential, commercial, industrial, and recreational zones.

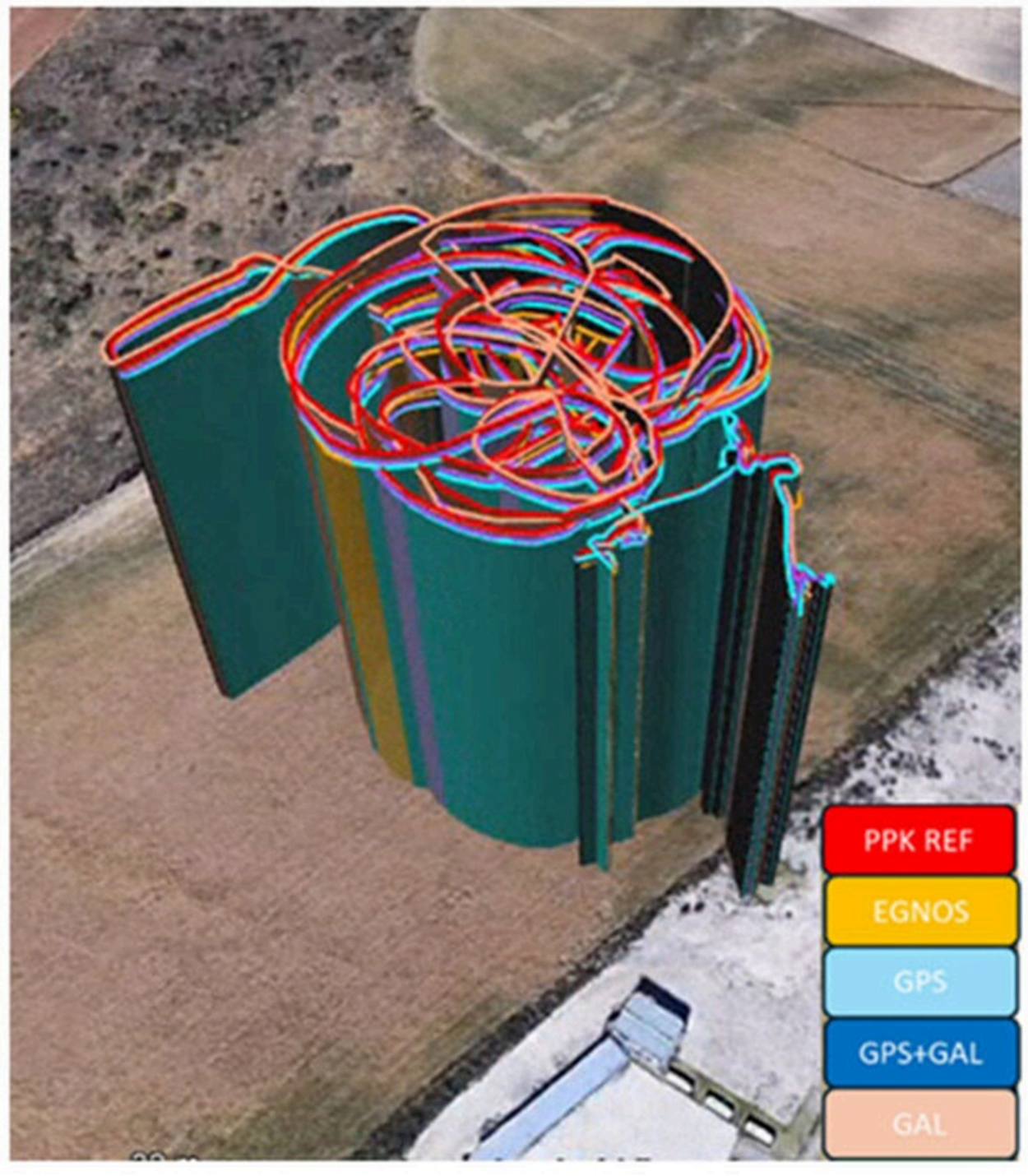

© 2023 The Author(s). | Published by Agro Intelligence Research Press

Figure 11. High-dynamics flight experiment—premium-grade receiver across several GNSS position modes.

The ambient environment consisted of a fully unobstructed sky, no interference, no ionospheric perturbations, and an antenna mask angle set to 0°. Across its 47-minute span, the sortie involved abrupt directional reversals and aggressive banking. This illustrates a taxing flight regime, in which the drone's angular orientation repeatedly blocks satellite signals from reaching the antenna.

The figures logged by the premium-grade receiver are presented for multiple GNSS position mode setups: SBAS/EGNOS, GPS Standalone (L1/L2), GPS + GAL (L1/L2 + E1/E5), and Galileo (E1/E5). The corresponding Horizontal and Vertical Position Error (HPE/VPE) outcomes are assembled in **Table 8**.

Table 8. High-dynamics flight. Premium-grade receiver across several GNSS position modes.

Parameter		High-end receiver			
		Galileo	GPS + GAL	GPS	EGNOS
HDOP (P95)		1.74	1.17	1.94	2.11
VDOP (P95)		4.2	2.01	2.43	2.89
NSV used (mean)		9.77	16.27	8.7	8.14
C/N_0 mean [dB-Hz]		38.79	40.26	41.72	42.26
HPE [m]	Max	8.71	6.21	12.62	8.17 [1]
	P95	3.63	2.18	3.91	1.40 [1]
	Mean	1.69	1.01	1.66	0.64 [1]
HPL [m]	Max	885.78 *	4544.41 *	3526.56 *	1000
HPE-HPL [m]	Max	−877.07	−4538.2	−3243.94	−991.83
Hacc [m]	Max	101.64	23.36	283.54	113.82
	P95	26.15	17.07	20.19	4.48
	Mean	8.57	4.64	7.66	2.34
Hacc-HPE [m]	Max	92.93	17.15	270.92	105.65
VPE [m]	Max	24.08	5.97	25.72	15.13 [1]
	P95	4.98	2.53	4.02	2.18 [1]
	Mean	2.03	1.01	1.46	0.92 [1]
VPL[m]	Max	4278.15 *	9136.1 *	3394.57 *	1000
VPE-VPL [m]	Max	−4254.07	−9130.13	−3368.85	−984.87
Vacc [m]	Max	78.47	370.07	35.9	173.29
	P95	30.04	15.14	18.57	5.84
	Mean	8.82	6.35	4.97	2.65
Vacc-VPE [m]	Max	54.39	364.10	10.18	158.16

© 2023 The Author(s). | Published by Agro Intelligence Research Press

Int. Monitoring Alarm	N/A	N/A	N/A	808
MI detected	0	0	0	0

* The PL values displayed were not computed in conformity with the DO-229 methodology. [1] Disregarding epochs where an integrity monitoring alarm remained actively raised.

This experiment constitutes a representative case of a typical UAS mission in which the vehicle, together with its GNSS antenna, executes rapid rotations and steep rolls. Although the external environment does not match the severity of those characterised in the preceding sections, the flight manoeuvres themselves degrade the receiver's output. The evaluation indicates that the premium-grade unit yielded higher Protection Levels and greater Position Errors, directly resulting from these flight dynamics. The unit raised 808 alarms during EGNOS tracking, recording zero MI events, and thereby gave the operator notice that the GNSS-derived position may have become unreliable. Satellite geometry worsened uniformly across all tested configurations, driving HDOP/VDOP metrics upward while altering the count of usable satellites. Additionally, C/N0 readings dropped below those observed during the nominal flight.

Conclusion

This study brings to the forefront the obstacles encountered when one seeks to apply the SORA 2.5 High Level Requirements to a GNSS, and it presents the outputs harvested from a suite of GNSS data gathering exercises spanning disparate settings, documenting the divergences between a disturbance-free nominal baseline and conditions where multiple degradation sources compromise GNSS performance.

As discussed in Section 2, SORA 2.5 provides that OSO#13 applies solely to external services whose continued availability is vital to flight safety. In the concrete case of treating GNSS as an external service, one cannot universally label it critical across the entire spectrum of UAS architectures, since some designs rely on alternative positioning sources as their primary navigation means. Nonetheless, it is important to note that the overwhelming majority of commercially marketed UASs adopt a fusion architecture that pairs a GNSS sensor with an Inertial Navigation System (INS) sensor, typically unified by an Extended Kalman Filter (EKF). In such setups, the need for GNSS depends on the drift properties of the chosen INS sensor and the time remaining before the mission concludes. For Micro Electro Mechanical System (MEMS) INS sensors, drift rates tend to be considerable, accumulating meaningful offsets within short time spans. Determining whether the GNSS element is critical necessitates a tailored, case-by-case assessment of each UAS architecture, and this determination lies within the remit of the UAS operator.

Where the design assessment concludes that GNSS is indeed critical to flight safety, OSO#13 imposes two parallel duties: first, to articulate the minimally acceptable performance level; and second, to continuously track the service while the mission is in progress, both of which apply to SAIL III and higher-risk specific category undertakings. It follows that a methodology for gauging the performance of such external services must be settled upon. The fundamental complication of treating GNSS as an external service stems from the fact—amply illustrated in Section 3—that its real-world performance is shaped jointly by the quality of the SiS, by the characteristics of the sensor that computes the position fix from those signals, and by the operating environment, which exerts a dominating influence over positioning accuracy. Multiple candidate metrics exist for tracking the service during flight, all of which are elaborated in Section 3: these include VDOP, HDOP, NSV, C/N0, estimated accuracy, and HPL/VPL. As the tabulated outcomes from the experiments in this study reveal, indicators such as DOP, NSV, and C/N0 can offer some clues about the GNSS state. Still, they lack the fidelity to indicate when the GNSS signal is degrading reliably. They are consequently unsuited to serve as the trigger mechanism for alerting the pilot or autopilot, or for launching a predefined contingency response.

Take, for example, DOP—a metric that describes the spatial arrangement of the satellites being tracked—which might tempt one to infer that favourable geometry (i.e., low DOP) guarantees correspondingly strong positioning output. In practice, however, DOP furnishes no supplementary information when degradation sources such as ionospheric

© 2023 The Author(s). | Published by Agro Intelligence Research Press

disturbance or multipath arise. Even when VDOP and HDOP appear perfectly acceptable, as documented in Sections 3.1.2 and 3.1.3, the resulting positioning quality falls markedly below that achieved under the nominal scenario.

On a different front, there is a distinct category of metrics suited to tracking positioning performance that simultaneously accounts for service provision, the sensor, and the external environment. These are the estimated accuracy and the pair of Horizontal Protection Level (HPL) and Vertical Protection Level (VPL). As the experimental findings demonstrate, the estimated accuracy metric fails to remain above the PE at every epoch when the GNSS signal deteriorates. Even under those very same degraded conditions, Protection Levels derived under the stricter implementations of DO-229 manage to bound navigation errors throughout the operation, providing an alert when the Protection Levels exceed the accuracy threshold required by the operation. It should be noted that DO-229 stops short of requiring Fault Detection (FD) functionality for every category of user and operation; however, within the context of this work, an integrity monitoring detection mechanism has been assumed to operate at every epoch. Accordingly, such Protection Levels can be leveraged to alert the pilot or to invoke whichever mitigation measures are necessary to safeguard operational safety (for example, commanding a switch to a different navigation mode).

A range of receiver models was employed across the experimental campaign, and the PL values produced rest upon two fundamentally different computational approaches. For the premium-grade unit in the EGNOS configuration, the computation method follows the DO-229 standard; for both the intermediate-grade unit and the premium-grade unit's other operational configurations, however, the computation method departs from that standard. As the results clearly show, the premium-grade receiver can flag degradation events and raise an alarm when the PVT solution becomes untrustworthy. The intermediate-grade unit, on the other hand, demonstrated that MI events occur under signal degradation. This means that during some epochs, the actual positioning error—determined later through post-processing—is larger than the PL figure computed at that same epoch, indicating that the system was not equipped to issue an alarm. Such figures might be pressed into service as a rough benchmark of the error one might anticipate in a benign setting. Yet, they cannot be treated as genuine Protection Levels suitable for high-risk UAS missions. A deeper investigation into why these PL values fail to bound the positioning error reliably is not feasible, given that the manufacturer withholds technical details about the specific algorithm used to generate them.

As the results of the varied experiments reveal, the PL values produced by the premium-grade unit in accordance with DO-229 effectively prevent MI events, though their absolute magnitudes lean toward the substantial. In particular, under nominal conditions **(Table 1)**, the separation between the PL and the actual positioning error reaches 12 m, and this gap widens to nearly 1 km in degraded scenarios **(Table 4)**. Divergences of this scale are excessively large for UAS missions beyond the SAIL III level, where the demanded positioning performance is expected to remain within metre-scale tolerances—such precision being necessitated by the fact that these missions are anticipated to unfold within more tightly bounded spaces. The root of this issue lies in the standard's origin: it was conceived for manned aviation (with an integrity risk allocation of 10^{-7}), a context in which values of this magnitude satisfy the criteria applicable to those categories of aircraft and operations. Beyond that, the standard was formulated under the assumption of open-sky conditions, relying upon SBAS corrections applied to GPS L1 alone. For UAS platforms navigating settings that depart from open-sky conditions—where terrain contours or man-made structures can obscure the GNSS signals—the observable count of GPS satellites can drop substantially, thereby limiting what the system can deliver. Given this reality, turning to multi-constellation solutions in such settings is invariably recommended to boost the number of visible satellites.

Furthermore, the straightforward importation of this standard into the UAS sphere risks narrowing the types of operations that can be conducted. In high-risk contexts, where the UAS is moving through confined spaces—think urban streetscapes or clusters of buildings—these elevated PL values will act as an operational constraint. With this in mind, and cognisant of the PL computation algorithms currently available, the formulation of a new, purpose-built PL standard tailored specifically to UASs is strongly recommended.

Beyond the points raised above, while SAIL III operations have already been conducted in some European states and their frequency is widely anticipated to climb, it is notable that the GNSS sensors presently available on the commercial

© 2023 The Author(s). | Published by Agro Intelligence Research Press

market have not yet incorporated PL computation following DO-229 (this observation applies especially to intermediate-grade and consumer-grade receivers). The use of the estimated accuracy parameter, supplemented by a safety margin intended to contain the positioning error, offers a practically viable pathway for monitoring GNSS service provision within medium-risk specific category contexts (SAIL III), at least for the interim period until a wider selection of commercial receivers adopts genuine Protection Levels.

To conclude, the evidence collected across a spectrum of scenarios—spanning stationary experiments in impaired environments to dynamic experiments free of degradation—has shown that GNSS cannot be treated as a generic, interchangeable sensor, since a wide array of factors shapes its behaviour, any number of which can bring about a loss of operational control (depending upon the UAS's specific architecture and the criticality assigned to the GNSS component). This reality makes it necessary to monitor such systems during operations to identify when performance falls below the standard required for flight safety, thereby issuing an alarm that notifies the UAS operator or activating the appropriate mitigations. In the authors' view, implementing real-time monitoring of GNSS navigation performance through the triad of Protection Levels, Alert Limits, and Time To Alert will become indispensable to sustain operations beyond the SAIL III level.

The present investigation is circumscribed by its dependence upon PL computations anchored either to the DO-229 standard or to proprietary algorithms of undisclosed design sourced from various GNSS manufacturers, and by the finite set of scenarios examined. For these reasons, future research should focus on experimental verification across a broader palette of operational and environmental conditions, as well as side-by-side comparisons across differing PL algorithms—work that would buttress the conclusions advanced in this study. Finally, the development of integrity algorithms purpose-built for the UAS domain, capable of dialling back the conservative margins inherent in the DO-229 approach without compromising the requisite safety thresholds, is urgently advocated.

Acknowledgements

The authors would like to thank the Eurocae WG-105 SG-6 members who collaborated on the development of this work, enabling the space to discuss and review the topic and providing valuable feedback.

Conflict of interest

This work was carried out within EUROCAE WG-105 SG6 DP007, in collaboration with various companies and public entities. L.M.G.-d. and D.S. were employed by Telespazio Ibérica SLU. ESSP SAS employed J.B., E.L., M.S., R.G., and E.G. GMV Aerospace and Defence S.A.U employed G.M. S.H. was employed by the Institute of Robotics, BAS. The EU Agency employed J.K. for the Space Programme (EUSPA). Skyeton Germany GmbH employed M.V. DLR Gesellschaft für Raumfahrtanwendungen mbH employed J.G.. EUROCONTROL Innovation Hub employed P.H., and NAV CANADA employed S.R.B. The authors declare that the research was conducted in the absence of any commercial or financial relationships that could be construed as potential conflicts of interest.

Financial support

None

Ethics statement

None

Received: 21 May 2022 Revised: 26 Jul 2022 Accepted: 11 Aug 2022

© 2023 The Author(s). | Published by Agro Intelligence Research Press

Published online: 25 November 2023

Rights and permissions

Open Access The author(s) retain copyright. This article is licensed under the Creative Commons Attribution-NonCommercial-ShareAlike 4.0 International License. It may be shared and adapted for non-commercial purposes with appropriate attribution, an indication of changes, and distribution of adaptations under the same license. Third-party material may be subject to separate terms identified in its credit line. View the license at https://creativecommons.org/licenses/by-nc-sa/4.0/.

References

1. IndustryARC. Unmanned Aerial Vehicle Market to Reach $69.9 Billion by 2030. https://www.industryarc.com/PressRelease/3900/unmanned-aerial-vehicle-market (accessed on 22 September 2025).

2. Grand View Research. Commercial UAV Market to Reach $41,781.7 Million by 2030. https://www.grandviewresearch.com/press-release/commercial-uav-market-analysis (accessed on 22 September 2025).

3. Bijjahalli S, Sabatini R, Gardi A. Advances in intelligent and autonomous navigation systems for small uas. Prog Aerosp Sci. 2020;115:100617.

4. Donato V, Moccardi A, Conte C, de Alteriis G, Accardo P, Federico M, et al. A High Precision Aerial Indoor AI-Based Inspection System. In: Proceedings of the 2025 IEEE 12th International Workshop on Metrology for AeroSpace (MetroAeroSpace). Naples, Italy; 2025. p. 81-6.

5. Turci L, Crispino G, Causa F, Opromolla R, Orsolillo L, Corraro F, et al. Performance Assessment of LiDAR-Visual-Inertial Fusion for GNSS-Resilient Aerial Navigation. In: Proceedings of the 2025 IEEE/ION Position, Location and Navigation Symposium (PLANS). Salt Lake City, UT, USA; 2025. p. 924-34.

6. Maigualema-Quimbita DA, Melero VM, Gomez-Barquero D, Tejedor JVB. Positioning of Unmanned Aerial Vehicles (UAVs) in Urban Environments Using 5G Networks: A Hybrid Approach Based on Multilateration and Machine Learning. In: Proceedings of the 2025 Integrated Communications, Navigation and Surveillance Conference (ICNS). Brussels, Belgium; 2025. p. 1-9.

7. Sorbelli FB, Conti M, Pinotti CM, Rigoni G. UAVs Path Deviation Attacks: Survey and Research Challenges. In: Proceedings of the Annual IEEE Communications Society Conference on Sensor, Mesh and Ad Hoc Communications and Networks Workshops. Como, Italy; 2020.

8. Navipedia (ESA). Navigation Integrity. https://gssc.esa.int/navipedia/index.php/Integrity#cite_note-2 (accessed on 22 September 2025).

9. RTCA. RTCA DO-229: Minimum Operational Performance Standards (MOPS) for Global Positioning System/Satellite-Based Augmentation System Airborne Equipment. https://standards.globalspec.com/std/14281994/rtca-do-229 (accessed on 22 September 2025).

10. Huang Z, Mou W, Wang R, Li P, Lyu Z, Ou G. A Survey of GNSS Receiver Autonomous Integrity Monitoring: Research Status and Opportunities. Front Phys. 2025;13:1567301.

11. Yang F, Wang E, Pang T, Qu P, Zhang Z. Research on RAIM Algorithm Based on GPS/BDS Integrated Navigation. In: Lecture Notes in Electrical Engineering. Singapore: Springer; 2017;438.

12. Zhang M, Qin P, Zhang M, Chen P. ARAIM Algorithm Performance on UAV Platforms in Urban Areas. In: Lecture Notes in Electrical Engineering. Singapore: Springer; 2023;845.

© 2023 The Author(s). | Published by Agro Intelligence Research Press

13. Fu L, Zhang J, Li R, Cao X, Wang J. Vision-Aided RAIM: A New Method for GPS Integrity Monitoring in Approach and Landing Phase. Sensors. 2015;15:22854-73.

14. Nam G, Kim J, Min D, Lee J. Along-track position error bound estimation using kalman filter-based raim for uav geofencing. J Position Navig Timing. 2023;12:51-8.

15. EASA. Specific Operations Risk Assessment (SORA). https://www.easa.europa.eu/en/domains/drones-air-mobility/operating-drone/specific-category-civil-drones/specific-operations-risk-assessment-sora (accessed on 22 September 2025).

16. JARUS SORA 2.5. http://jarus-rpas.org/publications/ (accessed on 22 September 2025).

17. Eurocae. Eurocae WG-105 SG-6 SORA. https://www.eurocae.net/working-group/wg-105-sg-6/ (accessed on 22 September 2025).

18. EASA. Operating a Drone. https://www.easa.europa.eu/en/domains/drones-air-mobility/operating-drone (accessed on 22 September 2025).

19. EASA. Means of Compliance (MoC) for the Design of UAS Operated in SAIL III. https://www.easa.europa.eu/en/document-library/product-certification-consultations/means-compliance-moc-design-uas-operated-sail (accessed on 22 September 2025).

20. EUROCAE. WG-105 SG-6 ED-280: Guidelines for UAS Safety Analysis for the Specific Category (Low and Medium Levels of Robustness). https://www.eurocae.net/product/ed-280-guidelines-for-uas-safety-analysis-for-the-specific-category-low-and-medium-levels-of-robustness/ (accessed on 22 September 2025).

© 2023 The Author(s). | Published by Agro Intelligence Research Press